ANALYSIS OF RESERVOIR PROPERTIES OF FAULTED AND FRACTURED EOLIAN THRUST-BELT RESERVOIRS

by
Dustin Keele and James Evans
Department of Geology, Utah State University, Logan, Utah

OPEN-FILE REPORT 529
UTAH GEOLOGICAL SURVEY
a division of
Utah Department of Natural Resources
2008

ANALYSIS OF RESERVOIR PROPERTIES OF FAULTED AND FRACTURED EOLIAN THRUST-BELT RESERVOIRS

by

Dustin Keele and Jim Evans

Cover Photo: Outcrop of Jurassic Navajo Sandstone, Grand Staircase-Escalante National Monument, southern Utah. Photo by Sonja Heuscher.

Disclaimer

OPEN-FILE REPORT 529
UTAH GEOLOGICAL SURVEY
a division of
Utah Department of Natural Resources
2008

Analysis of Reservoir Properties of Faulted and Fractured Eolian Thrust-Belt Reservoirs

Dustin Keele and James Evans
Department of Geology
Utah State University, Logan, Utah 84322-4505

EXECUTIVE SUMMARY

We examined the sedimentary and structural petrography and petrology of the Jurassic Nugget Sandstone, northeastern Utah and southwestern Wyoming, as sampled by 3 cores in Anschutz Ranch East field. Approximately 2700 ft of core from three wells were logged and sampled for petrographic analyses, and these data were combined with existing porosity and permeability data to determine the relationships between lithology, depositional setting, diagenesis, and the style of deformation.

Anschutz Ranch East field lies in the hanging wall of the Absaroka thrust, and consists of an asymmetric anticline in the Jurassic Nugget Sandstone. All of the rocks examined fall within the subarkose to quartz arenite fields. We identified four facies types in the Nugget at Anschutz Ranch East: dune, apron, dry interdune, and wet interdune. Dune facies are interpreted as having been deposited in an erg setting, and are characterized by very fine to medium-grained sandstones with high-angle, cross-strata and low amplitude ripples. Diagenetic and pore-filling characteristics include calcite nodules, carbonate-rich horizons, desert varnish, Fe-staining, and oil staining. Apron facies rocks represent an erg-sand sheet environment, and consist of very fine to medium-grained sands with high- to low-angle cross-strata, horizontal bedding, and low-amplitude ripples. Diagenetic and pore-filling characteristics include calcite nodules, carbonate-rich horizons, desert varnish, and oil staining. Dry interdune deposits are interpreted as having been deposited in a sand sheet environment, with silt to very fine sand grains, horizontal beds, and low-amplitude ripples. Hematite staining represents the dominant fluid-rock interaction. Wet interdune sequences were likely deposited in a standing water sabkha to very moist interdune setting. These rocks consist of silt to very fine sand-sized grains, with soft-sediment deformation, bioturbation, thin horizontal laminae, and trough cross-strata. Diagenetic features include carbonate-rich beds and hematite staining.

Deformation style is largely controlled by the primary depositional setting of the rocks. The high porosity dune facies sands tend to produce deformation bands, in which porosity and permeability are greatly reduced. The wet interdune facies produce open fractures and breccias, and the dry interdune and apron facies produce open to closed fractures.

Compilation of the core log data with permeability-porosity data available from the Utah Division of Oil, Gas and Mining website shows that primary depositional processes play an important role in the porosity and permeability of the rocks. When we plot the petrophysical data in k-n space, and correlate with the depositional setting inferred from the petrography, we see that the wet interdune facies have the lower k-n values, dry interdune and apron facies are intermediate, and dune facies the highest permeability and porosity.

When coupled with the nature of control on deformation, we suggest that deformation styles produce an inverse relationship where high porosity sands tend to produce deformation bands, the low k-n rocks have open fractures and breccias, and the intermediate facies produce open to closed fractures.

Net (2003) shows that the Nugget Sandstone at Anschutz Ranch East lost porosity primarily through mechanical compaction. Cements and pore filling observed in core samples show that diagentic pore fluids were patchy and that oil occupies the dune facies rocks in complex deformation band and cement bounded regions.

Taken together, the results of this study have significant implications for exploitation of oil and gas, or for CO_2 sequestration. Permeabilities in eolian sandstones in structurally complex regions will be a function of the primary depositional setting, diagenetic history, and the structural setting of the rocks. Permeability values may range over 3-4 orders of magnitude, resulting in heterogeneous flow and rapid break through or significant compartmentalization.

INTRODUCTION AND SIGNIFICANCE

Eolian strata constitute attractive exploration targets for aquifers, hydrocarbon reservoirs, and CO_2 sequestrations sites. However, depositional and diagenetic heterogeneities can greatly influence fluid-flow properties; thus there will be a preferred flow direction (Fig. 1). Furthermore, given the variations in deformation styles between porous and non-porous rocks (Nelson, 2001), depositional and diagenetic heterogeneities may influence the type of structural compartmentalization (Fig. 1). Despite significant advances in the scientific community and industry, answers to questions about rock strength and their relationship to primary sedimentological character remain elusive. This research illustrates how sedimentologic and diagenetic heterogeneities control the strength of eolian rock and, ultimately, to control fluid-flow properties of the rock.

Rock strength and structural position exert important controls on mechanisms of brittle deformation of rock. In sedimentary rocks, various sedimentologic and diagenetic heterogeneities such as grain size, bedding thickness, lithofacies, and types of cementation influence porosity. Primary rock characteristics control the porosity, and in turn, control the rheology and promote different types of brittle failure in sedimentary rock. Brittle failure in rock creates complexities by forming structural compartmentalization that overprints the stratigraphic and diagenetic characteristics in the rock body.

To develop a sound understanding of the factors that control the strength of eolian rock

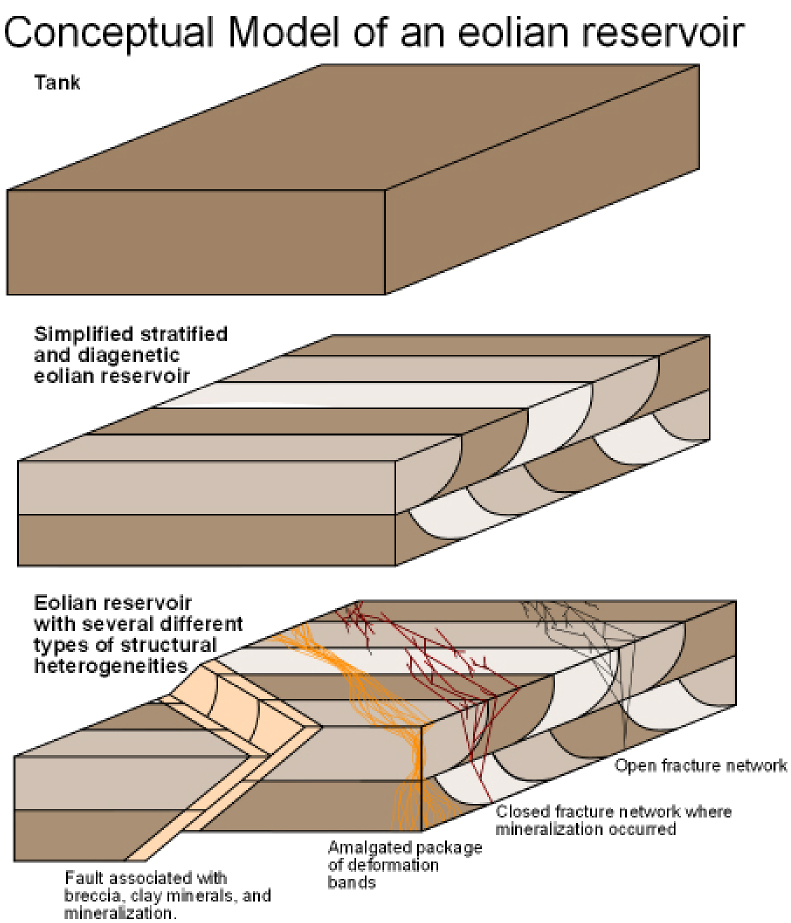

***Figure 1.** Eolian deposits are often considered to be a large tank that contains hydrocarbons. However, eolian deposits have two major controls on fluid flow: reservoir segmentation and permeability anisotropy. Interdune deposits and the basal portions of dune sets greatly reduce vertical communication. Horizontal flow may also be complicated by lateral variations in dune sets and cementation changes. Reservoirs that have experienced structural deformation have heterogeneities such as faults, deformation bands, and open-closed fracture networks that bring about further compartmentalization. Fluid is typically considered to travel parallel to faults, because of porosity reduction in zones of breccia. Deformation bands act more as a baffle, reducing permeability and not prohibiting fluid flow. Fracture networks that are closed generally prohibit fluid flow, while fracture networks that are open increase permeability. In effect, eolian rock packages that have experienced structural deformation have complex reservoir parcels that have different fluid flow characteristics.*

and its mechanical behavior in the subsurface, we examined the sedimentologic and diagenetic heterogeneities of the eolian Jurassic Nugget Sandstone from Anschutz Ranch East field, and the nature of the sedimentological features were defined and correlated with different types of structural deformation. Better understanding of eolian sandstone rheology will then lead to better methods in predicting types of deformation as a function of sedimentological architecture and diagenetic history.

The Nugget Sandstone in Anschutz Ranch East field provides an excellent opportunity to examine the relationship between petrologic characteristics and geomechanical processes that may lead to a better understanding of reservoir properties where a structural overprint is present. Anschutz Ranch East field is a large east-verging asymmetric anticline trap in the Utah-Wyoming thrust belt, situated along the northeast-southwest trending Absaroka thrust fault. Straddling the Utah-Wyoming border, the field is approximately 50 miles northeast of Salt Lake City, Utah (West and Lewis, 1982; Fig. 2).

Amoco Production Company extensively cored and collected well-bore based data from Anschutz Ranch East field in order to more accurately assess the *in-situ* fluid saturation of the reservoir and in the end have a better understanding of fluid flow properties in the field. While vast amounts of borehole data and other structural data were collected in the field, the data were poorly synthesized and have since been scattered across the United States.

Over the past 5 years, we located the core and a suite of conventional wireline logs and other subsurface data for Anschutz Ranch East field. Approximately 30,000 ft of core is stored at the Oklahoma Geological Survey in Norman, Oklahoma. Laird Thompson provided many of the petrophysical data in an electronic format for the program Petra® in addition to paper copies of many of the wireline logs. Porosity data were available from the Utah Division of Oil, Gas and

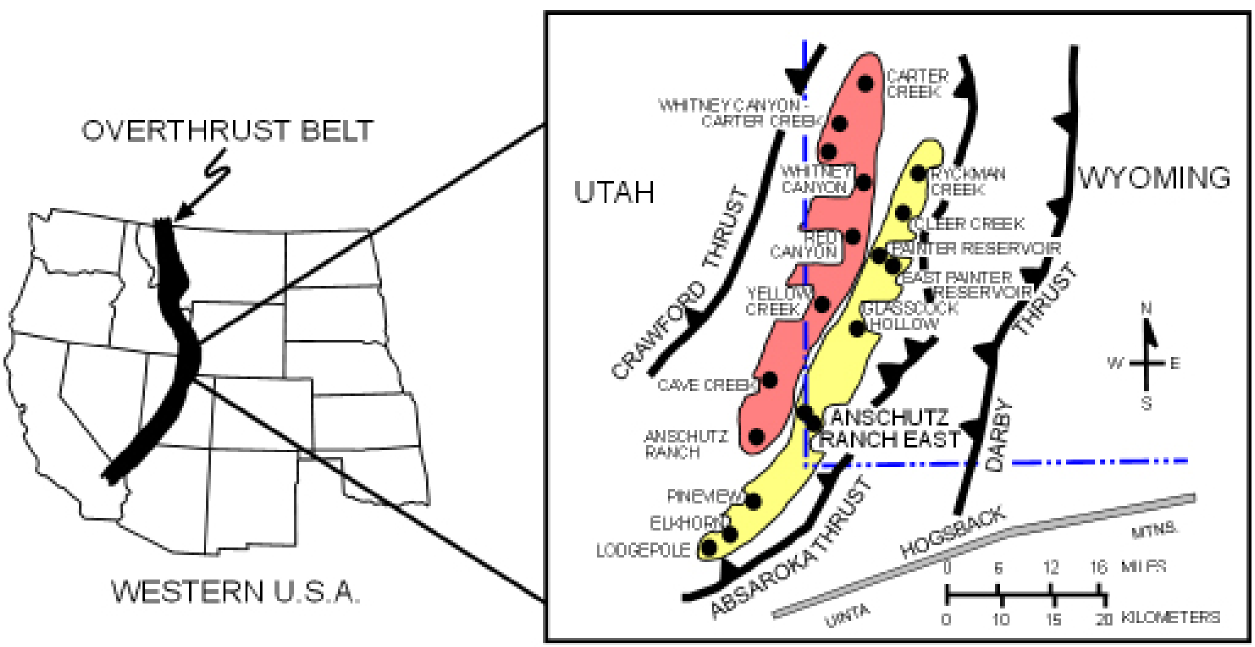

Figure 2. Location of the western Overthrust Province and Anschutz Ranch East field (indicated by an arrow) in the western United States. The enlarged image shows the major producing fields and hydrocarbon trends within the Utah-Wyoming segment of the thrust belt. Fields highlighted in pink produce sour crude. Fields highlighted in yellow produce sweet crude. Modified from Lelek, 1982.

Mining. These data were analyzed across the overturned anticline limb (the West Lobe) that forms the main structure in Anschutz Ranch East field, which illustrates how sedimentologic and diagenetic heterogeneities influence the type of brittle deformation in different structural positions.

This study also offers valuable knowledge on the development and the properties of fracture systems and deformation bands in the Utah-Wyoming fold-thrust belt. This investigation provides critical knowledge into the nature, evolution, and properties of mechanical deformation in eolian sandstone and can be used to improve understanding of faults, fractures, deformation bands, and brecciation.

PREVIOUS WORK

Anschutz Ranch East Field History

For many years the western overthrust belt has been an area of exploration activity. In 1969, one of the most recent and rigorous exploration periods began in the Utah and Wyoming overthrust belt when Amoco Production Company obtained an exclusive exploration agreement for the odd-numbered sections across the Union Pacific Railroad land-grant acreage (Dixon, 1982). Two productive trends soon became evident: an eastern “sweet gas and liquid trend” that produces primarily from the Nugget Sandstone and a western “sour gas trend” that produces from Paleozoic rock. In 1979, the Amoco Production Company discovered Anschutz Ranch East field, which lies within the eastern sweet gas and liquids trend (Lelek, 1982).

The discovery well penetrated 940 ft (286.5 m) of gross pay in the Jurassic Nugget Sandstone in what is now the West Lobe of Anschutz Ranch East field. The East Lobe was later discovered by the Anschutz Corporation at a much greater depth (White et al., 1990). Shortly after production in the West Lobe, the field was shut in until pressure maintenance could be fully sustained because reservoir pressure was so close to dew point pressure. In the East Lobe, sufficient differences existed between reservoir pressure and dew point pressure to tolerate partial pressure maintenance (cycling) and pressure depletion (White et al., 1990).

The West Lobe of Anschutz Ranch East field contains a rich retrograde gas-condensate with a dew point only 230 psi (1586 kPa) below the original reservoir pressure (White et al., 1990). Pressure depletion below the dew point would have resulted in condensate liquid drop-out of up to 40% of the hydrocarbon pore volume (HPV), and consequently a 75% loss of reserves in place (Kleinsteiber et al., 1983). This issue called for a specialized plan of maintaining reservoir pressure for optimized production. The specialized plan involved nitrogen injection to replace hydrocarbons produced from the reservoir. In order to get accurate reservoir modeling for a constant sweep, extensive coring of reservoir rock was completed to better predict the field’s response to various depletion schemes. In 1990, there were 30 producing wells and 18 nitrogen gas injection wells and production was expected to continue into the early part of the twenty-first century (White et al., 1990). The East Lobe entered its pressure depletion phase of production in the early 1990s (White et al., 1990). In the mid 1990s the field went through a series of purchases by several oil companies and corporate analysis; however, a complete reservoir analysis has never been completed (R. Nelson; L.B. Thompson, oral comm., 2005). In 2008, both the West and East lobes are largely operated by Merit Energy and there is some water flooding taking place in the West Lobe. The field appears to be in the “blowdown” phase. In some respects this study is a post-production analysis of the field. Results of this analysis might provide insights into how the sedimentology and structural geology combine to affect the flow properties of eolian sandstone reservoirs, which are of interest with the discovery of oil in central Utah.

Structural History

Anschutz Ranch East field, in northeast Utah and southwest Wyoming (Fig. 2), consists of two east-vergent asymmetric anticlinal closures: the West Lobe closure is in Summit County, Utah, while the East Lobe is predominately in Uinta County, Wyoming (Figs. 3 and 4). The field's anticlinal closures lie approximately structurally parallel and are situated within the Absaroka thrust sheet (Fig. 4). The Absaroka thrust sheet is one of the four major northeast-striking structural units to have thrust eastward during Cretaceous and Early Tertiary time, with thrusting along the Absaroka thrust probably culminating in Late Cretaceous time (Dixon, 1982; Lamerson, 1982; Lelek, 1982).

These anticlines formed on a ramp along the Absaroka fault plane (Warner, 1982; West and Lewis, 1982; Lelek, 1983; White et al., 1990; Lewis and Couples, 1993). The West Lobe is associated with the fault truncation of a Paleozoic carbonate succession and the East Lobe is associated with the truncation of a Mesozoic clastic/carbonate succession (West and Lewis, 1982; Warner, 1982; Lelek, 1983; White et al., 1990; Lewis and Couples, 1993).

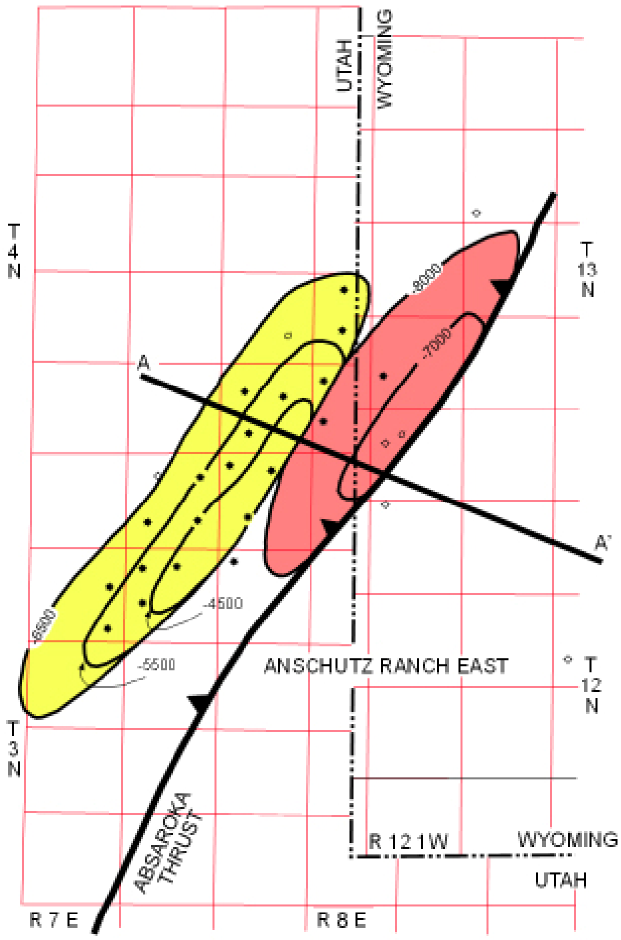

Figure 3. Generalized structure contour map of the top of the Nugget Sandstone in Anschutz Ranch East field. Contour interval is 1000 ft and A-A' is a structural cross section that can be seen in Fig. 4. The West Lobe is shaded in yellow, while the East Lobe is shaded in pink. Modified from West and Lewis, 1982.

Stratigraphy

The stratigraphy for the southern part of the Utah-Wyoming thrust belt is illustrated in Fig. 5, with the key productive intervals and potential source rocks indicated. The Paleozoic section is dominated by carbonate rocks, with the exception of some organic-rich Cambrian shale and the Pennsylvanian Weber Sandstone. The Woodside, Dinwoody, and Thaynes formations are the oldest rocks penetrated by wells and are only seen within the West Lobe of Anschutz Ranch East field. There are some variations within the Mesozoic and Tertiary sections although they generally consist of sandstone, siltstone, and shale with minor intermittent carbonate and evaporate strata. In Anschutz Ranch East field, the oldest rocks carried within the Absaroka thrust are probably the Triassic Ankareh Formation (thinly bedded siltstones and sandstones) (White et al., 1990), which lies conformably beneath the Nugget Sandstone and are the oldest rocks penetrated by wells in the East Lobe.

The Jurassic Nugget Sandstone is the

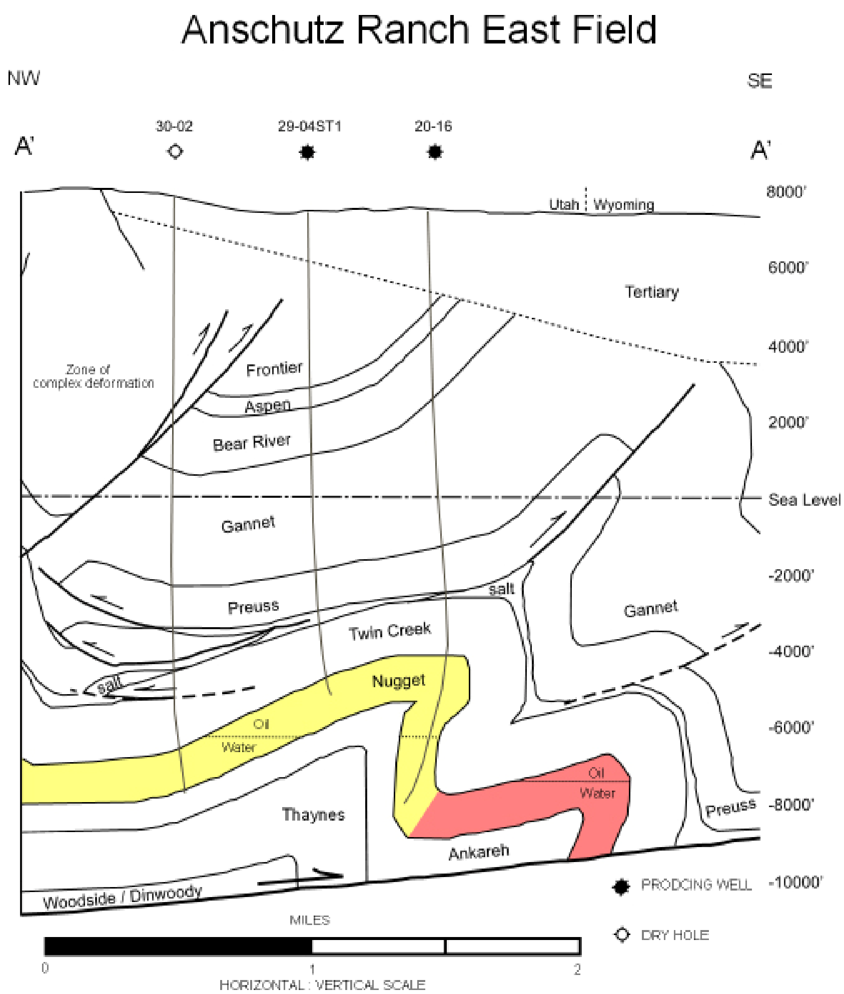

Figure 4. Generalized cross section of the Anschutz Ranch East field. The locations of the wells are projected onto the cross section. The portion of the Nugget Sandstone that is shaded in yellow is the West Lobe, while the portion that is shaded in pink is the East Lobe. See Fig. 3 for the location of cross section. Modified from West and Lewis, 1982.

primary hydrocarbon reservoir for the eastern sweet gas and gas condensate trend in Anschutz Ranch East field. The Nugget Sandstone is approximately 1050 ft (320 m) thick in the West Lobe and can reach depths of 14,700 ft (4480 m) (Lelek, 1982; White et al., 1990). The Twin Creek Formation overlies the Nugget Sandstone with a 1000-1500 ft (305-460 m) limestone sequence (Lelek, 1982; White et al., 1990).

There is commonly a detachment between the Nugget-Twin Creek package and the Upper Jurassic and Cretaceous formations in this portion of the thrust belt along thick Upper Jurassic salt lying beneath the Stump-Preuss sandstone and shale section. This salt interval is highly variable in thickness, thinning to as little as 7 ft (2 m) over the crest of the West Lobe and thickening to as much as 1200 ft (366 m) to the northwest along the back flank of Anschutz Ranch East (Lelek, 1982; White et al., 1990). The Stump-Preuss formations are overlain by the siliciclastic Cretaceous Gannet Group, which is overlain by the marine siltstone and shale of the Bear River, Aspen, and Frontier formations (Lelek, 1982; White et al., 1990). The Late Cretaceous to Tertiary Evanston and Wasatch formations locally unconformably overlie the Cretaceous section, with pronounced angularity (Fig. 5).

Sand Sea

During the Jurassic (190-180 Mya) the Nugget and Navajo Sandstones were deposited in part of the largest known ancient dune field in western North America (Fig. 6),

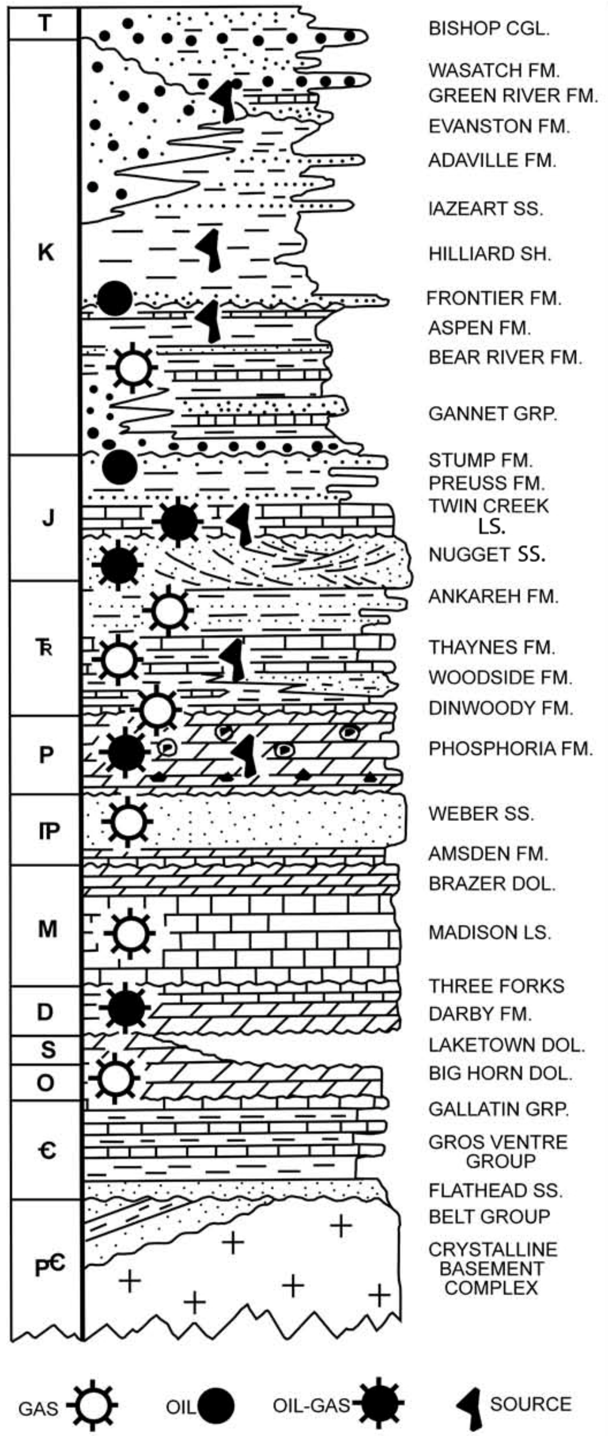

Figure 5. Generalized stratigraphy for the Utah-Wyoming thrust belt with producing reservoirs and potential source rocks indicated. Modified form White et al., 1990.

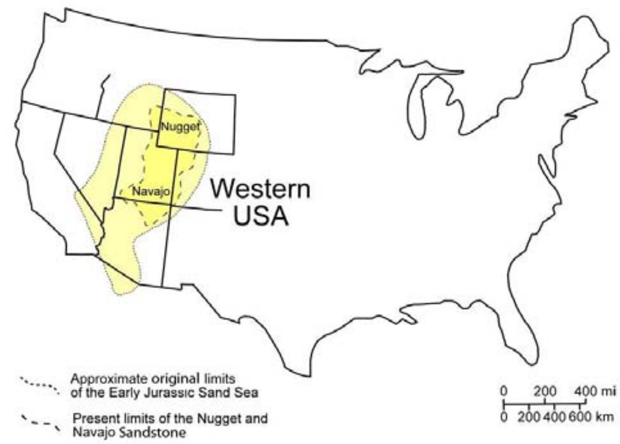

Figure 6. Map showing the original inferred extension of the Nugget/Navajo Sandstone and approximate original limits of the sand sea in the western US. Modified from Net, 2003.

covering a minimum estimated area of 22,728 miles^2 (36,600 km^2) at latitudes ranging from 15° to 25°N (Peterson and Pipiringos, 1979; Net, 2003). Regional tectonic and stratigraphic analyses indicate that the Nugget/Navajo thickness reached a maximum thickness of 2221.2 ft (677 m) in central Utah (Blakey et al., 1988; Net, 2003). Paleogeographic reconstructions reveal that the dominant sediment transport direction was to the south (Fig. 7) (Peterson, 1988; Loope et al., 2004). Deposits in the sand sea may have been transported from the uplifted central Montana area and vicinities, and possibly farther north from Canada, including recycling of late Paleozoic eolian units (Blakey et al., 1988). Blakey et al. (1988) suggest this additional reworking contributed to high textural and mineralogical maturity of the sediment.

Eolian Deposits

Eolian sandstone formations are lithified wind-blown sand deposits that accumulated along sea coasts or in vast deserts called *sand seas* or *ergs* (McKee and Bigarella, 1979). Because air is only about one-thousandth the density of water, eolian processes are very

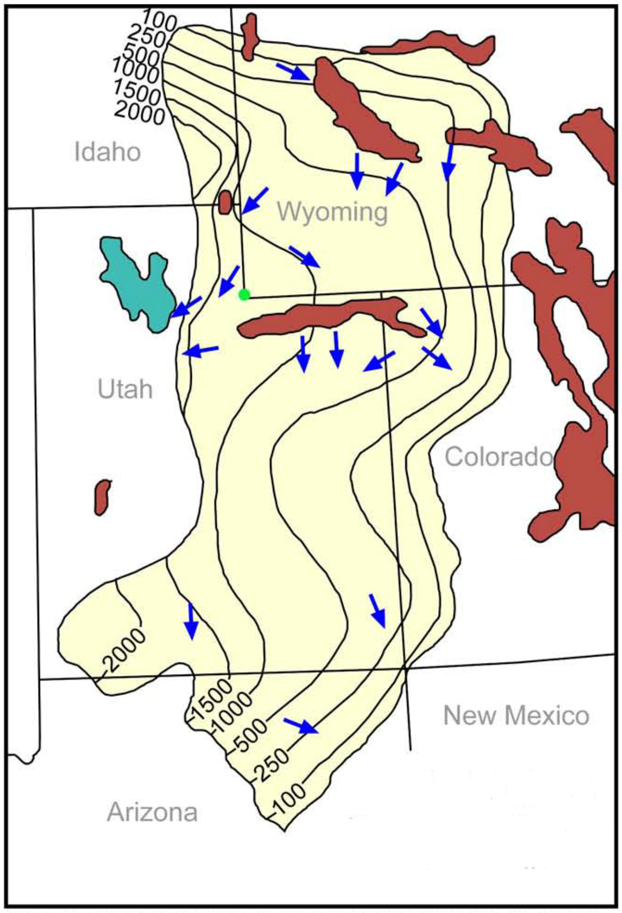

Figure 7. Isopach map of the Nugget and Navajo Sandstones. Laramide age structures are represented in red. Paleowind directions are indicated by the blue arrows (Doe and Dott, 1980; Doelger, 1987). Anschutz Ranch East field (green dot) is located within part of the thickest portion of the Nugget Sandstone. Modified from Jordan, 1965.

different from subaqueous processes and do not have the capability to transport coarse material. Eolian deposits are typically extremely well sorted, predominantly fine to medium-sized sand that occur in dunes and sand sheets and are carried by basal traction. Individual grains move by saltation and intergranular collision. Moderately to poorly sorted sand and other sediment types (e.g., carbonate) are found in interdunal areas. Adjacent to these eolian environments are other continental environments, such as alluvial fans, streams, lakes, sabkhas, or nearshore marine environments (Ahlbrandt and Fryberger, 1981, 1982; Morse, 1994). An eolian sequence is an amalgamated package of marginal dune deposits overlain by central dune or erg deposits capped by back-erg sands. Studies of modern dune fields show that the sedimentary structures in eolian deposystems include planar laminae, low-angle wind-ripples, grainfall laminae, and grain-flow cross-strata (Brookfield, 1977; Hunter, 1977; Lancaster, 1981; Mountney and Howell, 2000; Mountney and Thompson, 2002). Three of these facies types are commonly preserved in dunes and sand sheets in eolian sandstone (Kocurek, 1981). Dunes and sand sheets are identifiable and unique to specific processes in that environment; grain-flow (avalanching), grain fall (settling directly from the air after saltating off crests of dunes), or migration or translation of wind ripples on a dune surface (Kocurek, 1981; Morse, 1994). The distribution of eolian dune lithofacies can be seen in Fig. 8. The most notable eolian strata are large cross-strata formed by successive deposits on the lee side of sand dunes (Morse, 1994). Cross-strata in dune sets may be separated by nearly horizontal interdunal or toeset strata.

Interdunes are flat areas between dunes in which sand sheets, salt pans, or ponds may form (Morse, 1994). In dry interdunes, nearly horizontal erosional boundary surfaces are

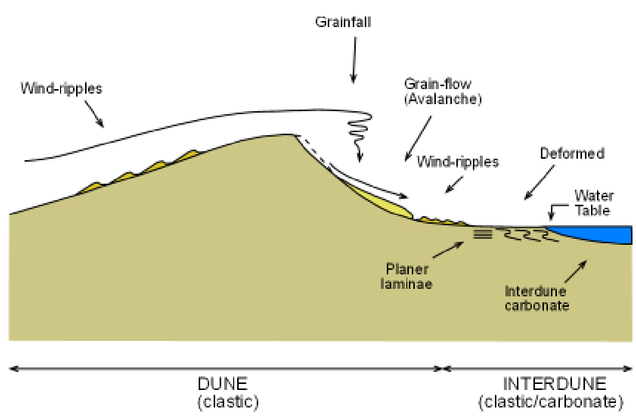

Figure 8. Schematic profile of an eolian dune showing the distribution of facies. See Table 1 for explanation. Modified from Net, 2003.

Table 1. Percentages of framework grains from well 30-02

Sample	Depth (ft)	Facies	Qm	Qp	K-spar	Plag	Alt K-spar	Ls	Lm	Lv	Lp	Zeolite
1	13125	Dune	70.27	9.91	19.37	0.00	0.00	0.45	0.00	0.00	0.00	0.00
23	13214	Dune	84.53	2.26	7.92	0.00	3.40	1.35	0.00	0.00	0.45	0.45
26A	13231	Dune	88.89	1.43	7.17	0.00	2.51	0.00	0.00	0.00	0.00	0.00
28	13248	Dune	85.54	0.40	10.04	0.00	3.61	0.45	0.00	0.00	0.00	0.00
48	13402	Dune	88.89	0.82	8.64	0.00	0.82	0.00	0.00	0.00	0.45	0.45
71	13763	Dune	90.18	5.96	3.16	0.00	0.35	0.45	0.00	0.00	0.00	0.00
29	13525	Apron	90.66	1.38	7.61	0.00	0.00	0.45	0.00	0.00	0.00	0.00
37	13299	Apron	82.46	3.51	10.88	0.00	2.11	0.45	0.00	0.00	0.90	0.00
44	13378	Apron	76.74	2.71	17.44	0.00	1.55	1.80	0.00	0.00	0.00	0.00
55	13631	Apron	81.02	3.65	12.77	0.00	2.55	0.00	0.00	0.00	0.00	0.00
64	13624	Apron	84.08	0.41	12.24	0.00	2.04	0.90	0.00	0.00	0.00	0.45
69A	13666	Apron	87.24	2.88	7.82	0.00	0.82	0.90	0.00	0.00	0.00	0.45
74	13800	Interdune (Dry)	90.43	0.71	6.74	0.00	1.06	1.35	0.00	0.00	0.00	0.00
75	13804	Interdune (Dry)	80.00	1.79	14.64	0.00	1.79	1.35	0.00	0.00	0.90	0.00
76A	13809	Interdune (Dry)	80.38	4.53	13.96	0.00	0.38	0.45	0.00	0.00	0.00	0.45
77	13860	Interdune (Dry)	91.32	1.04	4.86	0.00	1.39	1.80	0.00	0.00	0.00	0.00
82	13991	Interdune (Wet)	84.35	4.76	9.52	0.00	1.36	0.00	0.00	0.00	0.00	0.00
85A	14051	Interdune (Wet)	82.96	1.85	13.70	0.00	0.74	0.90	0.00	0.00	0.00	0.00
85B	14100	Interdune (Wet)	82.01	2.52	10.07	0.00	1.80	4.05	0.00	0.45	0.00	0.00
88	14112	Interdune (Wet)	81.71	0.41	10.98	0.41	2.03	4.05	0.00	0.00	0.45	0.45
90	14120	Interdune (Wet)	88.57	5.00	5.00	0.00	0.71	0.45	0.00	0.00	0.00	0.00

formed at the transition from highly dipping cross-strata to planar-laminae (Kocurek, 1981). In dry interdunal deposits where the water table is close to the surface, most if not all, sedimentary structures will be destroyed, creating a thick, massive bed (m scale) (M. Sweet, oral comm., 2005). In wet interdunes, poorly sorted sand, fine silt, clay, evaporate minerals, or limestone may be deposited (Morse, 1994). Interdunal deposits may also be disrupted by animals, roots, or salt (R. Oaks, oral comm., 2006).

Entrainment and transport of sediment by wind is strongly affected by the impact of moving grains hitting the bed. Saltation is the mechanism for producing wind-ripples. During saltation, sand-sized grains move by a series of jumps or hops, rising off the bed at a steep angle and then falling back along a shallow angle (Brookfield, 1977; Hunter, 1977; Lancaster, 1981). During grain-flow, cohesionless sediment is supported by dispersive pressure that has an internal flow regime and usually requires a steep slope. The mechanism for transport in grainfall is related to the settling of grains due to flow separation and deceleration at the crest of a dune (Brookfield, 1977; Hunter, 1977; Lancaster, 1981).

Nugget Sandstone Reservoir Properties

Lindquist (1983, 1988) and White et al. (1990) state that many of the reservoir properties of the Nugget Sandstone are tied to original depositional architecture and are only slightly altered by structural deformation and diagenesis. However, these authors don't address the extent of structural compartmentalization in Anschutz Ranch East field. It also appears that there is no previous work on correlating structural deformation with primary rock properties, which is addressed in this research.

Numerous authors (Lelek, 1983; Lindquist, 1983; White et al., 1990) have divided the Nugget in the West Lobe into three petrophysical zones (Fig. 9). The upper two-zones of the Nugget Sandstone contain large-scale eolian dunes and have the paramount reservoir rock, which is the richest pay zone. The lowest zone of the interval is characterized by interdune deposits; dry and water-influenced depositional textures, with some small-scale eolian deposits. This lower zone consists of the poorest reservoir rock in the Nugget.

The eolian sedimentary features have two major effects on fluid-flow: reservoir

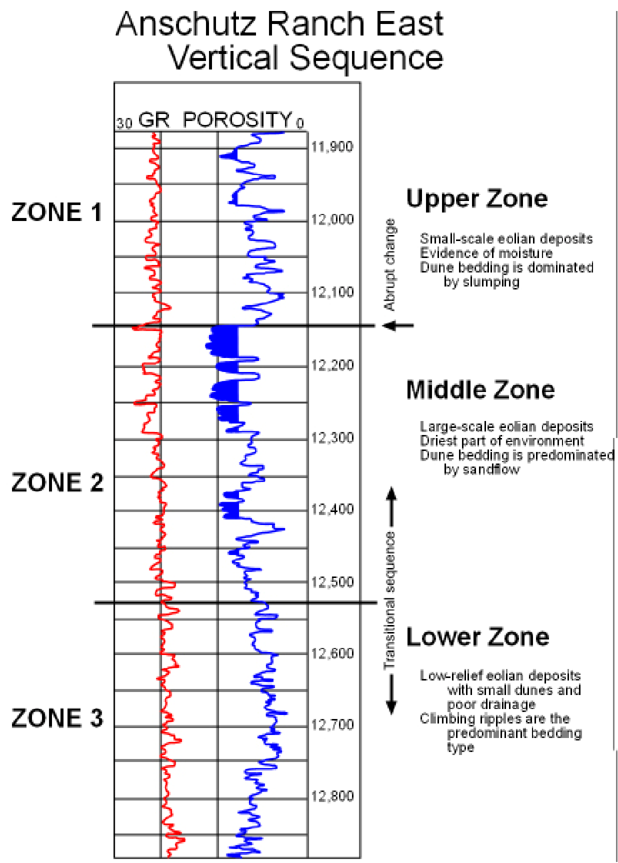

***Figure 9.** Typical gamma ray and calculated porosity log response showing the three zones of the Nugget Sandtone in Anschutz Ranch East field. The upper two zones of the Nugget contain the best reservoir rock quality. The porosity log is shaded blue at the values greater than 8%; the gamma ray log shows the decrease in shale content, or cleanliness of Zones 1 and 2. Major depositional characteristics are shown to the right of the log. Modified from White, et al. 1990.*

segmentation and permeability anisotropy (Lelek, 1983). There is a reduction in vertical communication by both interdune deposits and apron deposits, which have poor permeability. The horizontal flow may also be complicated due to the lateral variations within dune sets. There were prevailing northeasterly winds during the Jurassic, which resulted in a predominant southwest cross-bed dip in the Nugget Sandstone (Lelek, 1983; Peterson, 1988). In the subsurface this has been seen in both dip meter logs and core.

Rocks from Anschutz Ranch East field exhibit poor porosity and permeability correlations, especially when large intervals are considered (Lelek, 1983). The average pay zone porosity is 12% and the average horizontal permeability is 10 md (Lelek, 1983). In zone 1 of the Nugget Sandstone, permeabilities range from 0.5 to 10 md, while the porosities range between 7 to 15%, with water saturations from 13 to 50% (Bergosh et al., 1982). In zone 2, permeabilities range from 0.04 to 2 md, while the porosities range between 3.5 to 11.5%, with water saturations from 30 to 70% (Bergosh et al., 1982). In zone 3, the average permeability is 0.03 to 10 md, while the porosities range between 2 to 7%, with water saturations from 65 to 83% (Bergosh et al., 1982).

Diagenetic and structural processes are the principal phenomena that have affected the original reservoir quality. The most detrimental to reservoir quality are the quartz and feldspar overgrowths, especially near the bottom portion of the Nugget Sandstone, which can nearly obliterate any original pore space (Bergosh et al., 1982). Calcite nodules enclosing grains along cross-bed boundaries should not impede fluid-flow unless they coalesce to from impermeable streaks (Bergosh et al., 1982).

Diagenesis

An extensive study on the Nugget Sandstone diagenesis was completed by examining core taken from the Island Ranching No. 2 well, located on the backlimb of the West Lobe in Anschutz Ranch East field. Hematite staining and the formation of clay rims was most likely the first event that occurred (Bergosh et al., 1982). This was then followed by considerable dissolution of detrital grains and the precipitation of authigenic silica and carbonate cements that occurred under lithostatic pressure (Bergosh et al., 1982). Dissolved material was removed by migrating formation waters. It is likely that the authigenic silica cement was partly derived from the dissolution of grains and was then precipitated proximal to where the dissolution of grains occurred. Through the dissolution of K-feldspar and plagioclase, clay minerals and hematite were precipitated in the pore spaces of the sandstone. Sparry calcite is also a pore fill in the sandstone, however its appearance is patchy, isolated, and, in some places, concentrated along bedding planes or fractures. There are also trace amounts of ferrodolomite and authigenic quartz.

Within Anschutz Ranch East region, mechanical compaction and quartz cementation due to lithostatic loading during mesodiagenesis are the main diagenetic processes that the Nugget Sandstone has experienced (Net, 2003). The abundance and distribution of quartz cement is closely linked to clay rim distribution and burial temperatures (Wilson and Stanton, 1994; Net, 2003). The distribution of clay rims and quartz cements have an inverse relationship; in order for authigenic quartz to nucleate there has to be a clear surface (Net, 2003; Worden and Morad, 2003). Net (2003) showed that this has occurred within Anschutz Ranch East field in two wells that penetrated the Nugget Sandstone. Net (2003) also showed that the distribution of clay rims is directly related to lithofacies within an eolian deposystems.

HYPOTHESIZED SEDIMENTARY AND DIAGENETIC CONTROLS ON STRUCTURAL DEFORMATION

Almost all hydrocarbon reservoirs have some type of compartmentalization which develops due to brittle or ductile deformation and from primary stratigraphic or sedimentological controls (L.B. Thompson, oral comm., 2005). Understanding the influence primary sedimentological and diagenetic heterogeneities, such as the lithofacies and diagenetic history, have on certain types of deformation will aid in the prediction of fluid flow in deformed rock bodies.

1) Since eolian deposits are an amalgamated sequence of dune, apron, and interdune (dry and wet) facies and they have different geophysical properties, they should have different kinematics of structural deformation. Nelson (2001) states that bed thickness and changes in porosity affect the geomechanical behavior of sedimentary rocks. A working hypothesis was to determine if dune, apron, and interdune lithofacies will undergo different types of deformation. Different types of structural deformation will mean that each lithofacies has a different geomechanical behavior. If lithofacies has a control on the type of deformation, fracture networks and deformation band systems predictions based on wireline logs will have an increased success rate.
2) In well-sorted clastic rocks, decreasing grain size increases compressive and tensile strength (Nelson, 2001). This increase in strength is apparently a function of the grain surface area to grain volume ratio (Nelson, 2001). These observations were made qualitatively in clean quartz sandstone and it may be possible that other parameters besides grain size may control the strength of a rock. A working hypothesis of this study was that within coarser grain intervals, there would be a porosity increase; which would lead to a decrease in rock strength. This decrease in rock strength will promote an increase in the abundance of deformation bands.
3) Knowing whether interdunes were deposited in a wet or dry environment will greatly affect the type of deformation that may occur. Lindquist (1983) proposed that the interdunes in Anschutz Ranch East were probably dry to ephemerally damp. Sedimentary structures that are known to be present within interdune deposits include bioturbation, laminae, and deformed strata that are due to synsedimentary dewatering and slumping. It is also known that early cementation occurred, even further reducing the porosity within the interdune facies. It was hypothesized that there is a significant amount of brittle deformation that has occurred within interdune facies because of the extremely low porosity values and the overall thin bedding.

METHODS

Sampling

In order to evaluate the nature of the Nugget Sandstone in core, and to make correlations between lithology and deformation style, we focused on cores that would provide the widest range of structural settings and sampled the entire Nugget section. We focused on: 1) structural position in Anschutz Ranch East field, 2) the eolian facies, and 3) the diagenetic features in the core. The three cores that best fit the sampling needs are ARE well 20-16, located along the axial plane of the overturned anticline; ARE well 29-04ST1, approximately half-way up the backlimb; and ARE well 30-02, located near the base of the backlimb (Figs. 10 and 11). We selected ARE 30-02 because the entire interval of Nugget was cored and the well was a vertical borehole (Fig. 10). Well 29-04ST1 is a horizontal well (Fig. 10) and was chosen to investigate the extent of the lateral variations in deformation in the main sand interval of the reservoir. Since well 20-16 is within the axial plane of the anticline, differences in the type and extent of deformation based on tectonics and rock strength could be compared. Well 20-16 is slightly deviated, where it is projected along bedding (Fig. 10); this provided insight into the overall geometry of eolian deposystems. We studied 3490 ft (1064.5 m) of core for this study. Approximately 30,000 ft (9150 m) of core from the Anschutz Ranch East field is stored at the Oklahoma Geological Survey.

Core Logging Methods

Detailed analysis of core was conducted at the Oklahoma Geological Survey Core and Sample Library Lab in order to determine the facies architecture. Sedimentary structures are described using the nomenclature of Hunter (1977). Core-bedding attitude was measured (Fig. 12). Color of the rock was noted, along with diagenetic features including carbonate nodules, carbonate rich zones, bitumen staining, and oxidation fronts that may have moved through the Nugget Sandstone. Hydrochloric acid was used to determine whether carbonate cements are present. Along with the sedimentary and diagenetic features, structural deformation features were described while logging the core. Characteristics that represent aspects of the rock that might tend to increase fluid flow or compartmentalization were described and include deformation bands, breccias, faults, and fractures. Fracture types such as open, closed (mineralized), or fill (oil) were noted. The angle between bedding surfaces and deformational features was also measured.

Knowing whether a fracture has occurred naturally or whether it is drilling induced is critical in determining whether or not there is a relationship between structural deformation features and primary sedimentological and diagenetic features. The following conditions were used to indicate that associated fractures in core may have occurred naturally. Polished surfaces in well-lithified rock may be an

Anschutz Ranch East Field

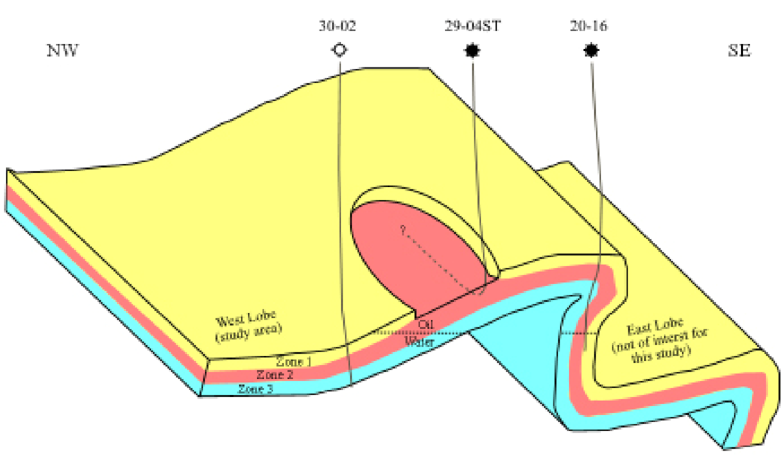

Figure 10. Projection of boreholes that were of interest for this study. The exact zones that well ARE 29-04ST1 penetrates are unknown. See Fig. 9 for explanations of each particular zone.

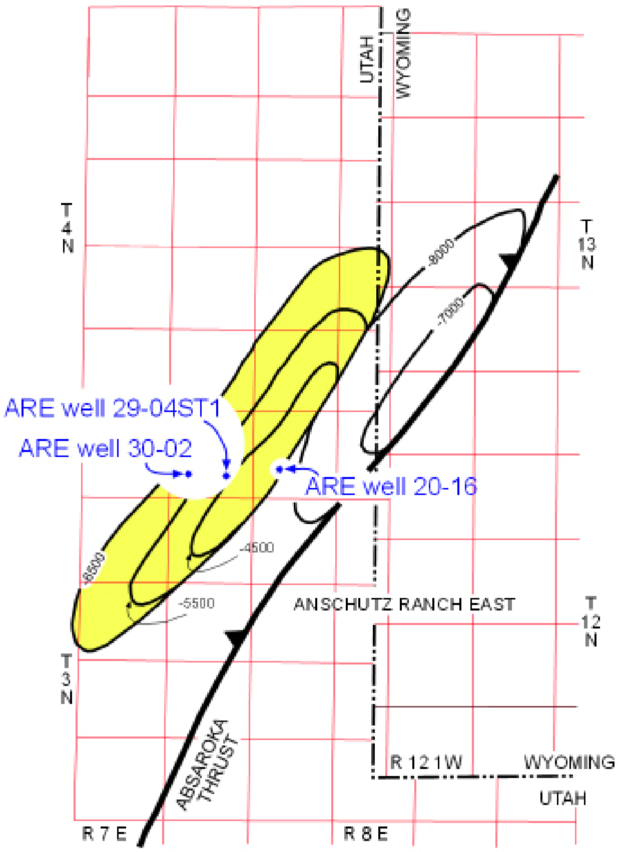

Figure 11. Generalized structure contour map of the top of Jurassic Nugget Sandstone, at Anschutz Ranch East Field. Contour interval is 1000 ft and the cores that were examined in this study are indicated in blue. The portion of the map that is shaded in yellow, is the West Lobe. Modified from West and Lewis, 1982.

indicator of natural fracture origin. Such surfaces are composed of slickenlines and slickenfibers (Kulander et al., 1990). However, polished surfaces, perpendicular to the core axis and accompanied by curved slickenlines, can be induced during the coring process (Kulander et al., 1990). Secondary mineralization and pressure solution features on walls of fractures will clearly indicate that fractures were naturally induced (Kulander et al., 1990).

Drilling-induced fractures commonly show a unique orientation within the core and are subparallel to the core axis (Kulander et al., 1990). The clockwise rotation of the drill bit may also cause chipping along the margin of the core, although natural fractures may also show this characteristic (Kulander et al., 1990). Also, overly damaged core that is stored may indicate rough handling at some point in the core's history.

Petrography and Statistical Tests

A total of 59 samples collected from areas of interest in the Nugget Sandstone core were made into thin sections. These thin sections were treated with a combination feldspar stain, which allowed for more accurate point counting. The combination stain contains Na-cobaltinitrite (yellow) and K-rhodizonate (pink) (Table 2). The intensity of the pink plagioclase stain is proportional to the amount of calcium in the molecule: albite/oligoclase will stain lighter than a more calcic plagioclase. Pure Na-albite will not take up any of the rhodizonate stain. Alkali feldspars are stained greenish-yellow. The accuracy of the stains decreases according to grain size: with finer grained specimens, the pink stain tends to pervade the surface and obscure the quartz grains.

The Gazzi-Dickinson point counting method was used to determine the mineralogy of each thin section. Point counting of thin sections was conducted to determine

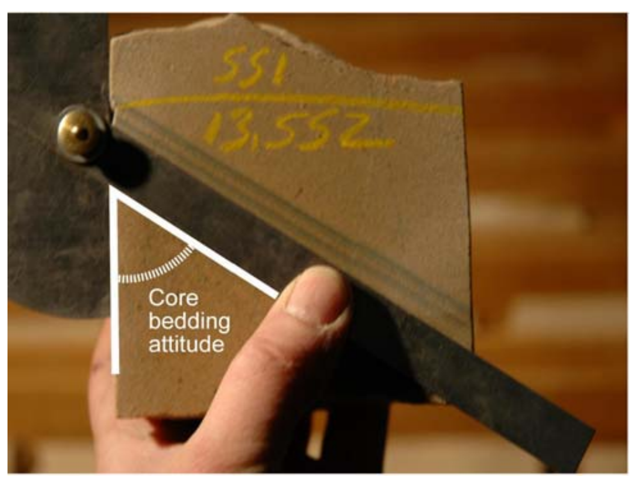

Figure 12. This figure shows how the core bedding attitude was measured for this study.

Table 2. Percentages of cement from well 30-02

Sample	Depth (ft)	Facies	Carbonate	Quartz	Hematite
1	13125	Dune	100.00	0.00	0.00
23	13214	Dune	57.58	39.39	3.03
26A	13231	Dune	40.00	60.00	0.00
28	13248	Dune	63.64	27.27	9.09
48	13402	Apron	14.29	71.43	14.29
71	13763	Apron	57.14	35.71	7.14
29	13525	Apron	73.33	23.33	3.33
37	13299	Dune	84.78	0.00	15.22
44	13378	Apron	82.35	11.76	5.88
55	13631	Apron	17.02	23.40	59.57
64	13624	Apron	74.29	14.29	11.43
69A	13666	Dune	25.00	66.67	8.33
74	13800	Interdune (Dry)	27.78	5.56	66.67
75	13804	Interdune (Dry)	0.00	31.58	68.42
76A	13809	Interdune (Dry)	40.00	60.00	0.00
77	13860	Interdune (Dry)	50.00	8.33	41.67
82	13991	Interdune (Wet)	100.00	0.00	0.00
85A	14051	Interdune (Wet)	48.28	10.34	41.38
85B	14100	Interdune (Wet)	71.43	0.00	28.57
88	14112	Interdune (Wet)	63.27	22.45	14.29
90	14120	Interdune (Wet)	37.42	0.00	62.58

mineralogy of 300 points per sample. This method requires that all grains sand size and larger be counted as their mineral type, rather than as a rock fragment. This assigns sand-sized crystals and grains within larger fragments to the category of crystal or grain, rather than to the category of the larger fragment (Ingersoll et al., 1984).

We modified the Gazzi-Dickinson point counting method to meet the specific needs of this project. All categories of grains and cement were counted except for pore spaces. This ensures that features which would help in identifying the diagenetic history were not overlooked.

Three categories of intergranular space were noted - grains, cements, and pore fillers. The grain category includes: monocrystalline quartz, polycrystalline quartz, potassium feldspar, plagioclase, sedimentary lithic, metamorphic lithic, volcanic plutonic lithic, altered potassium feldspar, and zeolite. The cement category includes: calcite, dolomite, quartz, and hematite. Since the thin sections were not stained with alizarin red-S to differentiate between carbonate cements, the only time dolomite cement was counted was when a rhomb landed under the cross hairs. Both calcite and dolomite can form rhombs, however dolomite is the most common. Doing this explains why Net (2003) has ferrondolomite as the dominate cement in the Nugget Sandstone in Anschutz Ranch East field. The pore filler category includes nimite (a chlorite group clay mineral), clay filling the pore space, clay rims, cataclasite, and dead oil.

From the 300 points that were counted in each thin section, lithological bulk compositions and grain weight percentages, cement weight percentages, and weight percentages of pore space fillers were determined. Determining these values allowed for an overall characterization of the rock.

Thin sections were also used to determine the complex diagenetic history of the Nugget Sandstone. The nature of cements was examined and used to determine how they affect structural deformation. By doing these steps, the diagenetic history could be determined and compared to other published interpretations.

X-ray Diffraction Methods and Geochemistry

X-ray diffraction (XRD) was used to determine the mineral composition of each sample and to determine the composition of the feldspars. Samples were crushed to a powder and then passed through a 125-mesh sieve. The sieved powder was packed in an aluminum cylinder and scanned from 5-65° at a speed of 0.04°per second. X-rays were produced with a copper tube at 40 amps with electrons accelerating at a potential of 45 Kv. Clay-fraction XRD analyses were also done on oriented clay slurries in deionized water dropped onto glass slides. Total organic content (TOC) was measured in oil rich samples using a modified method of Dean (1974).

Analysis of Conventional Wireline Logs

Wireline logs are routinely collected at almost all industry boreholes and are affected in one way or another by the presence of deformation features; however, they are seldom used in a systematic manner for analysis of structural deformation features. Interpretations of the wireline logs were correlated to the different types of structural deformation features seen in core. The conventional wireline logs that were used in this study are the dipmeter and caliper. We used the dipmeter tool to determine the orientation of bedding and in some cases deformation bands. We use the caliper logs to infer the presence of fractured zones. We also plotted the lithology along side the standard wireline data (e. g., Asquith and Krygowski, 2004) to show how the core data correlates with the wireline signatures.

Field Methods

We also examined an outcrop analog to develop a sense of how structures may be distributed beyond the wellbore scale. Outcrops in the Nugget Sandstone east of Bear Lake were chosen in structurally similar positions to the Anschutz Ranch fields. These rocks are exposed in a hanging-wall anticline of the Holmes Canyon thrust (Coogan, 1997) and are folded in a similar manner as the asymmetrical anticline of the West Lobe of the Anschutz Ranch East field. The best exposures are in South and North Eden Canyons. We examined outcrops of deformed Nugget to determine the depositional system and facies of the outcrop. This was accomplished by describing grain size, texture, and sedimentary structures using the nomenclature of Hunter (1977), and by mapping the sedimentary bounding surfaces and color. The types of brittle deformation were described and measured in the field. The primary structures at the field site included faults, fractures (open and closed), and deformation bands.

Petrophysical Reports

Analysis of petrophysical data allows us to quantify the porosity and permeability of the reservoir rocks, and to make correlations between porosity and lithology. Petrophysical data from Anschutz Ranch East field was obtained from a public source [http: // utstnrogmsql3.state.ut.us/UtahRBDMSWeb/main_menu.htm] for wells 30-02 and 16-20.

The core petrophysical reports were scanned and converted into an MS Excel format by optical character recognition (OCR). Once the core petrophysical report was in electronic format, verification of the electronic copy with the hard paper copy was conducted. When each core petrophysical report was in a spreadsheet format, contacts such as stratigraphic changes, lithological changes, fluid (oil/water), and even changes in structural deformation were identified and documented in each well. The use of drilling reports, mud logs, well test results, formation pressure data, and cores were also used in conjunction with core petrophysical report to guarantee that each contact is accurately located. Using borehole information for a well ensures that petrophysical data is grounded.

We show the porosity and permeability values (maximum values, 90° away from maximum, and vertical). Routine helium porosity values were measured on core plugs and ranged from 0 to 20%.

FIELD OBSERVATIONS

Outcrops of the Nugget Sandstone (Fig. 13) show that in the South and North Eden canyons (Plates 1 and 2) it is comprised of quartz-rich sandstone with sedimentary structures that compare favorably to those observed in modern dune sands and in ancient sandstones interpreted as eolian deposits (Hunter, 1977; Hunter, 1981; Kocurek, 1981; Kocurek and Hunter, 1986; Fryberger and Schenk, 1988). The presence of repetitive inverse-graded "pinstripe" laminae with inter-

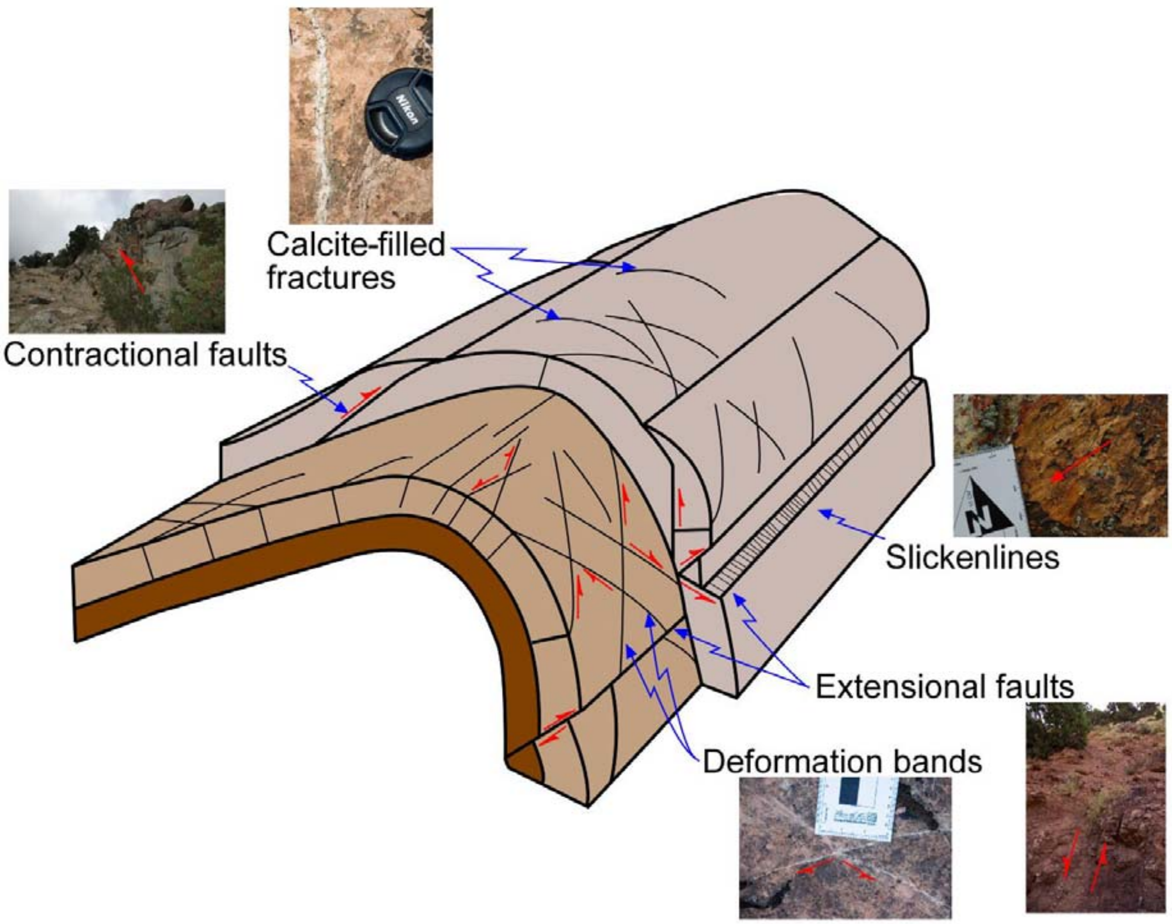

Figure 13. Schematic block diagram illustrating the principal mesoscopic deformational fabric elements North and South Eden Canyons: Bear Lake, Utah. All of the deformational features were seen in the Nugget Sandstone other than the extensional fault, which was only in the Gypsum Springs Member of the Twin Creek Limestone. Modified from Price, 1967.

bedded grainfall and grain-flow laminae are considered diagnostic of eolian sedimentation. Other more ambiguous sedimentary features that reflect an eolian depositional system include good sorting, non-erosive bases, types of hierarchical bounding surfaces, and meter-scale cross-bedding (Hunter, 1977; Fryberger et al., 1979; McKee and Bigarella 1979; Kocurek, 1981; Schenk, 1990). These strata are made up almost entirely by grain-flow and grainfall deposits, and low-angle ripples which represents a dune facies.

The goal of this fieldwork was to determine what deformational elements are most likely to occur within the Nugget Sandstone and their hierarchical development in the faulting process. On the mesoscopic scale, deformation in the Nugget is characterized by brittle failure in a strongly anisotropic rock. The deformational fabrics portray several distinctive types of planar to curved fractures and deformation bands.

Most of the tectonic fractures in outcrop are adjacent to faults. We observed hackle plumes, slickenlines, and well-developed calcite crystal coatings, some with slickenfiber textures that indicate a tectonic rather that unloading origin. Fractures (mainly open) form a fanning pattern with the slip direction suggesting the presence of a back thrust. Fault cores are relatively thin and the faulted rock is intensely fragmented. Fault cores diminish 3 to 6 ft (1-2 m) away from the slip surface, and the color distinction between host and faulted rock is prominent in the outcrop. In most cases, fault rock is lighter (whitish) in color and bounded by or contains slip surfaces that cut across individual bodies of fault rock. The slip surfaces are the most continuous fabric within the fault zone.

The density of fractures diminishes considerably outside of damage zone of faults. Deformation bands are also prevalent through much of the host rock and not always in close proximity to a fault. They are < 0.5 inch-wide whitish surfaces. Slip-surfaces are usually smooth to the touch, and in some cases show kinematic indicators (i.e., slickenlines) and have offsets on the scale of 0.118-0.394 inches (3-10 mm).

Overwhelmingly, deformation bands are perpendicular to bedding. Kinematically, deformation bands show a sense of shear with conjugate sets of deformation bands having angles around 40-50° between the bands. Bisector angles of these conjugate sets are perpendicular to major fold axis. This geometry correlates with the maximum compressive stress of the Sevier orogeny and is best described as a transverse deformational feature (Fig. 14) (Price, 1967; Salvini and Storti, 2004). Some deformation bands are

Figure 14. Two examples of compact multiple deformation bands in the steep limb of the Eden Canyon anticline.

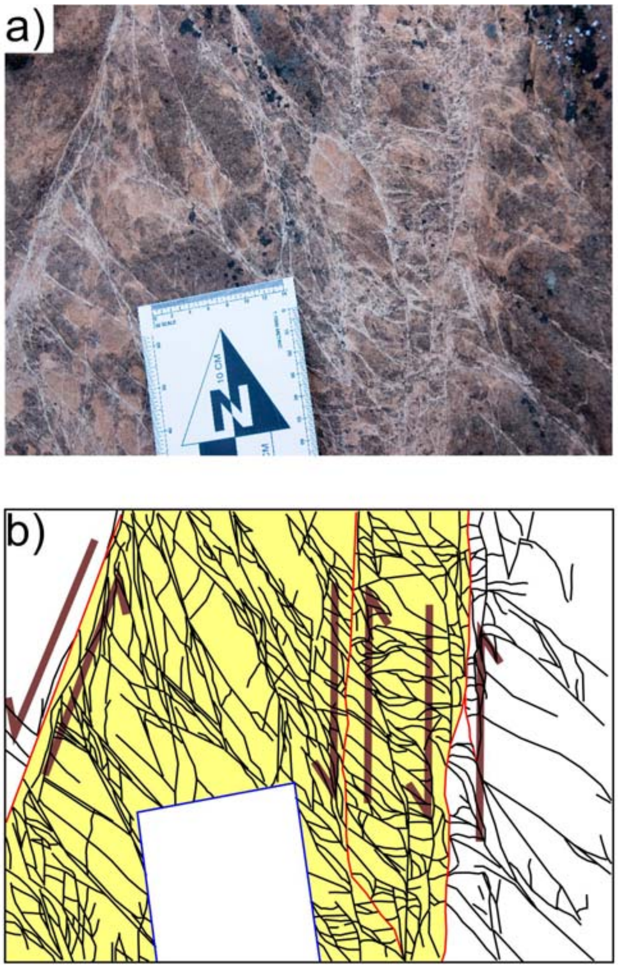

Figure 15. a). Outcrop photo and b) sketch of a ladder structure in the Nugget Sandstone in south Eden Canyon. Yellow – intact rock; red narrow slip zones; black lines indicate small connecting deformation bands.

parallel the fold axis, but they are certainly less abundant. These deformation bands that parallel the fold axis are longitudinal deformational features (Price, 1967; Salvini and Storti, 2004).

Numerous deformation bands also make up anastomosing systems (Fig.15) that commonly produce shear zones. Each of the deformation bands constantly interweave within the bounds of a narrow zone, Antonellini and Aydin (1994) referred to these systems as ladder structures (Fig. 15). The bounds of these shear zones can be designated by two main deformation bands which are linked by antithetic linking bands. The spacing between the stepovers appears to be closely related to the spacing between the two main shear zones features.

CORE DESCRIPTION

Facies and Reservoir Characteristics

The summary of the core-based descriptions, petrographic data, and petrophysical data are summarized in Plate 3. Analyses of the core reveals that in general, the relationship between facies and reservoir quality are closely linked (Plate 3) for the Nugget Sandstone in Anschutz Ranch East field. This is similar to that observed in other eolian fields (e.g., Auk field, described by Heward, 1991). Core descriptions, thin section analyses, and petrophysical data were combined to characterize the reservoir properties. The analysis presented in Plate 3 includes the detailed logging for facies and environments of deposition, nature and amount of cement, style of deformation, orientation of bedding, mineralization, and presence of oil. We show the results of permeability and porosity measurements made by CoreLabs in 1981 at confining pressure of 8000 psi (55158 pka), and the resulting graphical logs are distilled in the discussion below.

We identified four facies in Anschutz Ranch East field: dune, apron, dry interdune, and wet interdune. These facies were chosen for their distinct depositional characteristics and their ease of recognition in core. The highest quality reservoir occurs within dune facies, and a progressive deterioration is seen through apron to dry interdune facies. This reflects better sorting characteristics in dune sediments and a reduction in the proportion of sediment formed by fine-grained laminae. The poorest reservoir quality is displayed by wet interdune facies.

Sedimentary Structures

Diagnostic sedimentary structures observed in core of the Nugget Sandstone from Anschutz Ranch East field compare favorably with features observed in modern and ancient eolian sand deposits (Brookfield, 1977; Fryberger and Schenk, 1988; Hunter, 1977; Hunter, 1981; Kocurek, 1981; Lancaster, 1981; Mountney and Howell, 2000; Mountney and Thompson, 2002). Recognition of the inverse-graded, low-angle climbing ripples, horizontal beds, grain-flow and grainfall cross-stratification are key to the identification of dry eolian deposits (Hunter, 1981; Kocurek, 1981; Fryberger and Schenk, 1988). Recognition of low-angle and high-angle ripples can also be used as key diagnostic sedimentary structures (Fig. 16). A variety of sedimentary structures that are crucial in describing wet eolian deposits, such as soft-sediment deformation, bioturbation, high-angle ripples, and horizontal beds, trough cross-stratification, scoured surfaces, carbonated-rich horizons, and convoluted beds.

Diagenetic Features in Core

Major changes in the porosity and permeability of the Nugget Sandstone correspond with diagenetic features that are seen in core. Diagenetic features that correlate with specific facies are: calcite nodules, pervasive carbonate cementation, desert varnish, and hydrocarbon staining, and "zebra banding." In many cases diagenetic features such as hydrocarbon staining, "zebra banding," calcite nodules, and the presence of pervasive carbonates indicate the direction of maximum permeability.

Dune Facies

The dune facies consists mostly of brownish red to buff, well-sorted, fine- to medium- grained sands composed of high-angle cross-strata (Plate 3). Distinct planar cross-bedded foresets are dominated by steeply dipping, 20-37° (slabbed-face), and inverse graded avalanche deposits (Fig. 17). Individual grain-flow deposits can be difficult to identify, although occasional centimeter-scale tabular cross-sets are defined by millimeter-thick partings of finer grained grain-fall deposits. Grain-flow strata also occur interbedded with grainfall deposits, giving a "pin-stripe" lamination at slipface angles. In thin section, grain-flow and grainfall deposits show distinct differences in

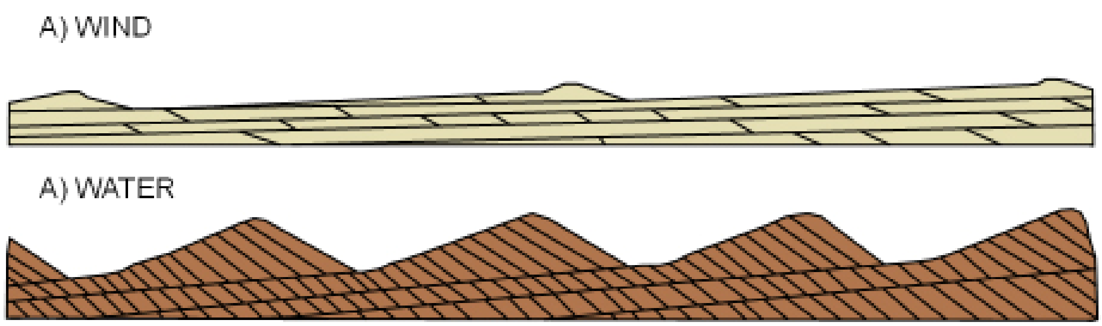

***Figure 16.** Contrasting climbing ripples translatent strata formed by migrating (A) wind ripples (low-angle) (B) and water ripples (high-angle). Wind ripples translatent strata are characterized by uniform, inversely graded laminae with few visible foresets. Wind ripples have a low amplitude, with coarser grains segregated to crests, and grains transported by saltation and creep. Water ripples have higher amplitude, segregation of coarser grains to troughs and well-developed foresets, which form by "mini-avalanches." Water ripples yield thicker, normally graded translated strata showing abundant foresets. Modified from Kocurek, 1981.*

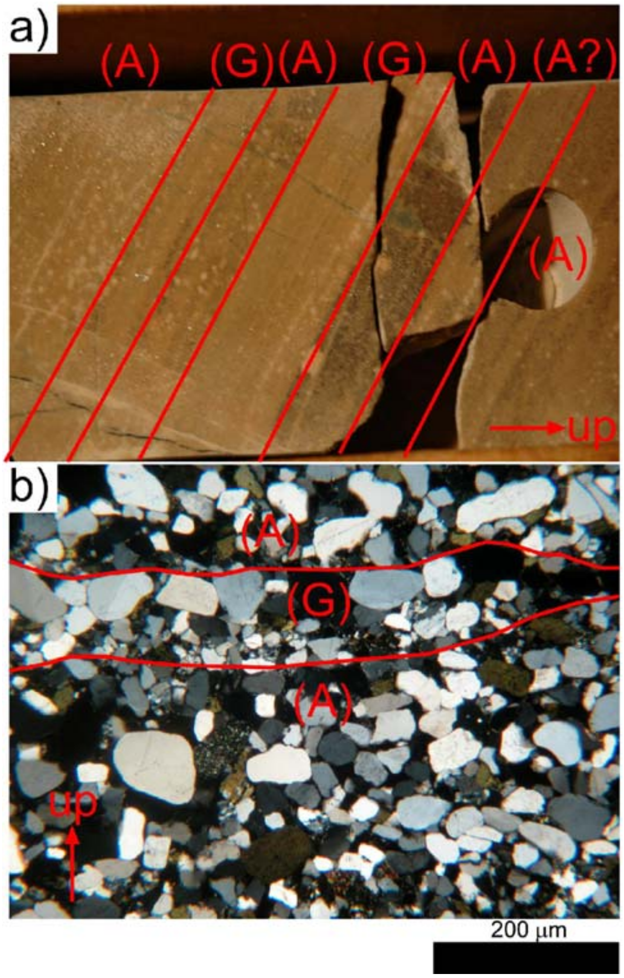

Figure 17. a) Core sample showing avalanche and grainfall deposits within a dune facies; Anschutz Ranch East well 30-02, (13,409 ft). The core sample was cut in half and the slab face is 10 cm across. Notice the bitumen staining that typically only occurs within avalanche deposits. b) Thin section showing avalanche (A) deposits and grainfall deposits (G), sample 20-16-33, (12,146 ft). Notice the bedding and grain size scale difference between these deposits in both core and thin

grain size and packing. Grain-flow deposits are relatively coarser grained and more loosely packed, whereas grainfall deposits are finer grained and relatively more tightly packed. Both deposits are well-sorted within distinct laminae. These sand laminae are interpreted to have been formed on the lee side of a dune. While low-angle ripples are not abundant within the dune faces, they are present.

These packages of rock are typically porous in well 30-02 (1.48-16.2%; average 10.46%) (Table 3). Coarser grained sands are commonly stained light grey to charcoal, giving a "zebra banding" appearance (Fig. 18) from hydrocarbons clogging pore throats (Fig. 19). In wells 20-16 and 29-03ST1, hydrocarbons have stained the majority of sand packages grey. This staining explains why these two wells are still producing, while well 30-02 was originally a gas injection well.

The diagenetic features that are descriptive of the dune facies are carbonate nodules that formed early in the diagenetic history of the Nugget Sandstone. Carbonate cements are common in the dune facies, typically within a single grain-flow deposit. This pervasive cementation most likely occurred with the nucleation of carbonate nodules. Desert varnish on grains is common. In well 30-02 at 13,559 ft (4135.5 m), desert varnish may have been extensive enough to reduce the porosity.

Apron Facies

Dune apron facies are typically brownish red to buff sequences of very fine to medium-grained sandstones, and are made up of low-angle ripples, high-angle cross-strata, low-angle cross-strata, and horizontal beds (Plate 3). Low-angle ripples are a distinct feature of the dune apron facies. Low-angle ripples result in a thin, essentially parallel stratification, which is inversely graded and millimeter scale (Fig. 20). Migration of low-angle ripples can occur on the stoss (upward) side of the dune or along the lee (downside) side of the dune due to reworking of former deposits by deflecting or reversing of wind directions (Brookfield, 1977; Hunter, 1977; Lancaster, 1981).

The apron facies is very common and marks the transition between the dune and dry interdune facies (Fig. 21). Laminae in the apron facies have variable bedding dips of 8-

Table 3. Percentages of pore fillers from well 30-02

Sample	Depth (ft)	Facies	Kaolinite	Illite	Cataclasite	Oil	Nimite
1	13125	Dune	0.00	100.00	0.00	0.00	0.00
23	13214	Dune	0.00	0.00	0.00	0.00	100.00
26A	13231	Dune	0.00	0.00	0.00	93.75	6.25
28	13248	Dune	14.29	28.57	0.00	0.00	57.14
48	13402	Apron	0.00	0.00	0.00	100.00	0.00
71	13763	Apron	0.00	100.00	0.00	0.00	0.00
29	13525	Apron	0.00	0.00	0.00	66.67	33.33
37	13299	Dune	0.00	0.00	36.36	9.09	54.55
44	13378	Apron	11.11	22.22	0.00	66.67	0.00
55	13631	Apron	0.00	50.00	12.50	0.00	37.50
64	13624	Apron	4.55	0.00	0.00	0.00	95.45
69A	13666	Dune	0.00	33.33	0.00	0.00	66.67
74	13800	Interdune (Dry)	0.00	0.00	0.00	0.00	0.00
75	13804	Interdune (Dry)	0.00	100.00	0.00	0.00	0.00
76A	13809	Interdune (Dry)	3.33	6.67	90.00	0.00	0.00
77	13860	Interdune (Dry)	0.00	0.00	0.00	0.00	0.00
82	13991	Interdune (Wet)	0.00	0.00	0.00	0.00	0.00
85A	14051	Interdune (Wet)	0.00	0.00	0.00	100.00	0.00
85B	14100	Interdune (Wet)	0.00	0.00	0.00	100.00	0.00
88	14112	Interdune (Wet)	0.00	40.00	20.00	40.00	0.00
90	14120	Interdune (Wet)	0.00	100.00	0.00	0.00	0.00

Figure 18. Bitumen staining "Zebra banding" is a very common diagenetic feature in the dune laminae. The staining is caused by hydrocarbons preferentially selecting individual grain-flow laminae, which have high permeability values, to travel through. Laminae that are not stained are grainfall deposits, which have lower fluid flow properties. Inter-bedding of grain-flow and grainfall deposits results in alternating fluid flow properties, thus, if hydrocarbons travel through the strata, bitumen staining only occurs within selected deposits. Anschutz Ranch East well 30-02 (13,446 ft).

20° (slabbed-face) (Plate 3), and inter-fingering between the dune face and interdune beds is common. Apron facies rocks are also typically high in porosity (0.5-14.9% in well 30-02; average 8.4%) (Table 3), however there are several low values. Also, the same diagenetic features that are seen in the dune facies are also common in the apron facies. However, low-angle ripples typically have not been stained by hydrocarbons, presumably because there is a significant anisotropy to flow properties (Hunter, 1977).

Dry Interdune Facies

Dry interdune facies are characterized by a brownish red to light brown sequence of very fine to medium sand grains, with abundant millimeter scale low-angle ripples and horizontal beds (Plate 3) (Hunter, 1977). Interdune facies have low sedimentary dips that range from 0–18° (Plate 3), which are probably due to the migration of ripples on

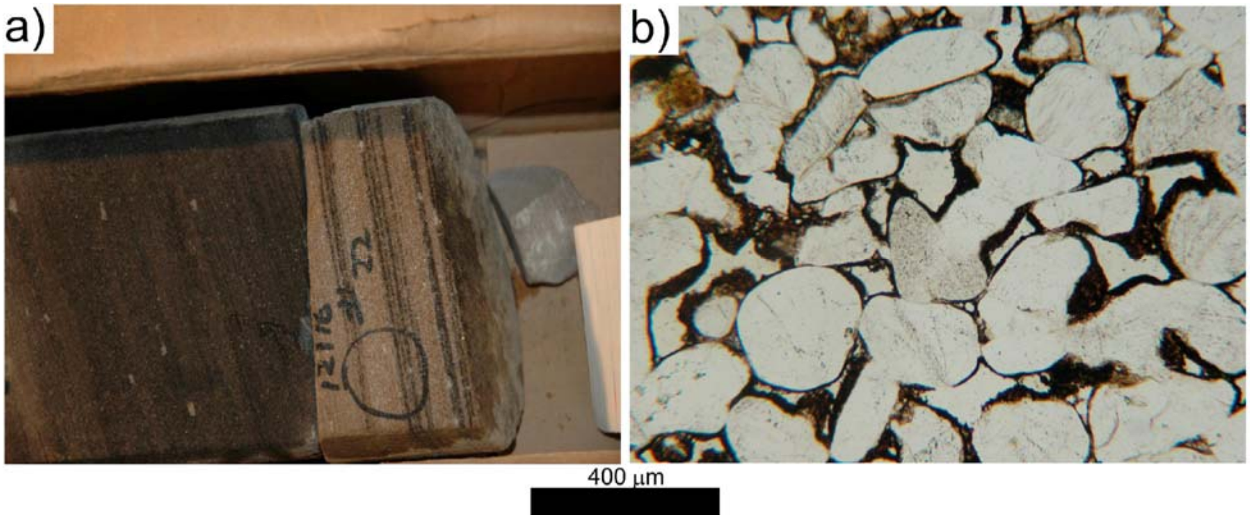

Figure 19 . a) Dune facies with extensive bitumen coating grains; Anschutz Ranch East well 20-16 (12,116 ft). The core sample was cut in half and the slab face is 10 cm across. b) Well-rounded quartz grains with bitumen coating most of the grains as many of the pore throats are clogged; sample 20-16-30 (12,116 ft).

Figure 20. Low-amplitude ripples result in thin, nearly parallel stratifications, which are inversely graded and millimeter scale; Anschutz Ranch East well 30-02 (13,380 ft). The core sample was cut in half and the slab face is 10 cm across.

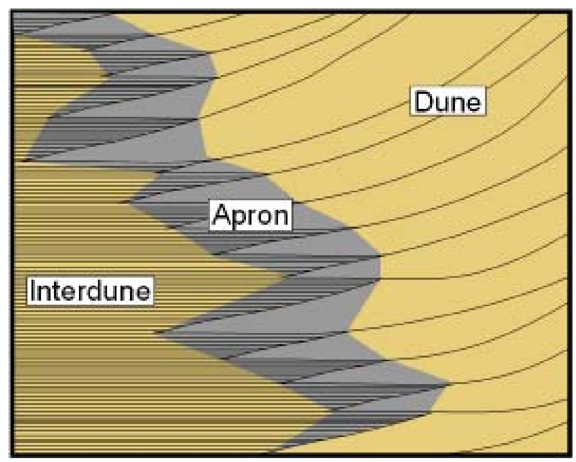

Figure 21. The inter-fingering between dune and interdune facies, which is very common in the Anschutz Ranch East field. This inter-fingering results in a gray area between these two facies, which causes difficulty in determining the exact facies in an interval of core. In this study, this transition zone is described as an apron facies. The apron facies does not have any distinct features other than that it is inter-fingering between dune and interdune facies.

the stoss and lee side of a dune (Kocureck, 1981). Migration of low-angle ripples results in an inversely graded, thin, essentially parallel stratification due to the translation of climbing ripples (Hunter, 1977).

Dry interdune facies are overall poorly sorted and tightly packed, which results in significant anisotropy of flow properties (Schenk, 1983). Overall values of porosity in dry interdune facies have a very large variability (0.01-9.69% in well 30-02; average 6.46%). The dry interdune facies generally does not have the same diagenetic features that dune or apron facies have. Instead, grains are commonly coated in illite and/or hematite. Hematite gives dry interdune facies its distinct color.

The features observed in this facies are similar to those described from modern sand sheets (e.g., Kocurek and Hunter, 1986; Sweet et el, 1988). Modern sand sheets are composed of broad areas of small dunes and extensive flats. Eolian sand sheets usually are found along the margins of dune fields where a high water table or early cements inhibit the formation of larger dunes (Kocurek and Hunter, 1986). In terms of reservoir properties, the sand sheet facies is characterized by a background of low permeability with thin, discontinuous, higher permeability packages of eolian dunal strata.

Wet Interdune Facies

The wet interdune facies consists mostly of brownish red to brown, poorly sorted, silt to fine-grained sandstone with high-angle ripples and horizontal beds (Plate 3). Other sedimentary structures distinctive of wet interdune facies include soft-sediment deformation and bioturbated planar cross-bedded foresets. Although interdune carbonate beds are not common and probably not volumetrically significant within this study area, their presence plays a vital role in determining transgression boundaries. Well 30-02 contains an interval [13,331-13,334 ft (4065-4067 m)] of interdune carbonate beds with 47% carbonate.

In well 20-16 [12,857-12,859 ft (3921.4-3922 m)], trough cross-stratification is present and reflects a relatively high-energy environment characteristic of channelized flow. Thus, an ephemeral stream is most likely the origin of this thin, high-energy deposit. The overall dip of beds is 0-18° on the slabbed-face of core (Plate 3). Convoluted beds and scoured surfaces suggest sheet flood rather than channel processes. Due to universally poor reservoir quality, wet interdune facies are all genetically lumped together.

Wet interdune facies are very poorly sorted and tightly packed due to bioturbation. Bioturbation destroys the sedimentary fabric and introduces fine sediment, resulting in an overall reduction in original porosity and significant anisotropy to fluid flow properties (Schenk, 1983). Net (2003) suggested that syndepositional dewatering probably was a large factor in porosity reduction, which is directly related to sorting and packing of clastic sediment.

Porosity in the wet interdune facies has a large variability (0.01-9.69% in well 30-02; average 6.46%). Wet interdune facies generally have the same diagenetic features that dry interdune facies have, although there is a large amount of hematite present. Clay minerals such as kaolinite and illite are common in thin section, presumably due to the alteration of minerals in a subaqueous environment. In the case of interdune carbonate beds, Ahlbrandt and Fryberger (1981) suggested that these rocks constitute effective internal barriers to fluid flow, potentially impeding hydrocarbon migration or isolating productive intervals in the subsurface.

ANALYTICAL RESULTS

In this study three cores were examined and samples were collected from distinctive lithologic units, diagenetic features, and deformational structures. Of the 190 samples that were collected, 59 were examined in thin section. There were 21 that were examined from well 30-02, 30 from well 16-20, and eight from well 29-04ST1. Point counts were made to determine percentages of framework (grains), matrix (pore fillers), and cement. Carbonate cement is the most prevalent cement in the Nugget Sandstone, however, in the lower portions (zone 3), silica cement prevails. Tables 1-10 show the data from these analyses.

Table 4. Percentages of framework grains from well 20-16

Sample	Depth (ft)	Facies	Qm	Qp	K-spar	Plag	Alt K-spar	Ls	Lm	Lv	Lp	Zeolite
15	11874	Apron	84.64	0.00	11.79	0.00	1.79	0.36	0.00	0.00	0.00	1.43
19	11946	Apron	92.96	1.41	3.87	0.00	1.06	0.70	0.00	0.00	0.00	0.00
20B	11972	Apron	91.80	3.13	2.34	0.00	1.56	0.39	0.00	0.00	0.39	0.39
22	11992	Apron	87.50	3.41	4.55	0.00	2.65	1.89	0.00	0.00	0.00	0.00
26	12063	Apron	84.94	1.26	12.13	0.00	0.42	1.26	0.00	0.00	0.00	0.00
30	12116	Dune	91.09	1.55	5.04	0.00	1.16	1.16	0.00	0.00	0.00	0.00
33	12146	Dune	79.79	1.05	11.15	0.00	5.23	2.79	0.00	0.00	0.00	0.00
34	12147	Dune	78.45	1.41	10.95	0.35	4.59	2.83	0.35	0.35	0.35	0.35
41	12222	Apron	83.78	2.03	9.12	0.00	2.70	1.01	0.00	0.00	0.00	1.35
43	12341	Dune	94.40	1.49	1.49	0.00	1.87	0.37	0.00	0.00	0.00	0.37
44	12351	Apron	88.93	1.79	6.43	0.00	1.79	0.71	0.00	0.00	0.00	0.36
46	12432	Dune	87.93	2.07	6.21	0.00	0.69	0.34	0.00	0.00	1.38	1.38
48B	12468	Interdune (Dry)	85.20	0.80	12.00	0.00	0.40	0.00	0.00	0.00	0.80	0.80
50A	12500	Apron	87.28	1.41	6.36	0.00	3.18	1.06	0.00	0.00	0.00	0.71
59A	12710	Interdune (Wet)	81.88	0.72	12.68	0.00	3.26	1.09	0.00	0.00	0.00	0.36
61A	12742	Interdune (Wet)	82.94	0.40	15.87	0.00	0.79	0.00	0.00	0.00	0.00	0.00
51B	12811	Apron	88.14	2.03	7.80	0.00	0.68	0.00	0.00	0.00	1.02	0.34
54B	12857	Interdune (Wet)	77.45	4.00	15.64	0.73	0.73	1.09	0.00	0.00	0.36	0.00
53B	12872	Dune	84.59	0.00	11.47	0.72	2.51	0.00	0.00	0.00	0.00	0.72
57	12903	Interdune (Wet)	78.60	0.00	20.16	0.00	1.23	0.00	0.00	0.00	0.00	0.00
63B	12979	Apron	82.97	0.36	13.77	0.00	1.81	1.09	0.00	0.00	0.00	0.00
1	13050	Apron	78.15	1.48	14.81	0.00	2.96	2.59	0.00	0.00	0.00	0.00
28B	13067	Interdune (Wet)	76.57	2.29	18.29	0.00	1.71	1.14	0.00	0.00	0.00	0.00
2	13073	Apron	70.67	1.41	22.97	0.35	2.47	1.77	0.00	0.00	0.35	0.00
5	13125	Interdune (Wet)	75.56	2.59	16.67	0.37	1.48	2.96	0.00	0.00	0.00	0.37
8	13186	Interdune (Dry)	84.15	2.03	9.35	0.00	0.00	2.85	0.00	0.00	0.41	1.22
12	13244	Interdune (Wet)	75.89	3.90	16.31	0.00	1.42	2.13	0.00	0.00	0.35	0.00
74	13521	Apron	88.26	6.06	4.55	0.00	1.14	0.00	0.00	0.00	0.00	0.00
75	13527	Apron	77.69	2.39	18.73	0.00	0.80	0.40	0.00	0.00	0.00	0.00
77	13574	Dune	83.52	1.83	12.09	0.00	0.73	1.83	0.00	0.00	0.00	0.00
80	13653	Apron	83.87	1.79	12.54	0.00	1.43	0.36	0.00	0.00	0.00	0.00

Table 5. Percentages of cement from well 20-16

Sample	Depth (ft)	Facies	Carbonate	Quartz	Hematite
15	11874	Apron	78.57	0.00	21.43
19	11946	Apron	80.00	10.00	10.00
20B	11972	Apron	71.43	0.00	28.57
22	11992	Apron	56.00	0.00	44.00
26	12063	Apron	68.42	0.00	31.58
30	12116	Dune	33.33	0.00	66.67
33	12146	Dune	25.00	0.00	75.00
34	12147	Dune	37.50	12.50	50.00
41	12222	Apron	55.56	44.44	0.00
43	12341	Dune	77.78	0.00	22.22
44	12351	Apron	42.86	50.00	7.14
46	12432	Dune	75.00	25.00	0.00
48B	12468	Interdune (Dry)	25.00	6.25	68.75
50A	12500	Apron	100.00	0.00	0.00
59A	12710	Interdune (Wet)	50.00	45.00	5.00
61A	12742	Interdune (Wet)	65.85	17.07	17.07
51B	12811	Apron	100.00	0.00	0.00
54B	12857	Interdune (Wet)	95.65	0.00	4.35
53B	12872	Dune	60.00	40.00	0.00
57	12903	Interdune (Wet)	72.22	9.26	18.52
63B	12979	Apron	69.57	30.43	0.00
1	13050	Apron	66.67	26.67	6.67
28B	13067	Interdune (Wet)	89.43	0.00	10.57
2	13073	Apron	21.43	78.57	0.00
5	13125	Interdune (Wet)	60.87	34.78	4.35
8	13186	Interdune (Dry)	36.11	38.89	25.00
12	13244	Interdune (Wet)	41.18	47.06	11.76
74	13521	Apron	94.74	5.26	0.00
75	13527	Apron	62.50	37.50	0.00
77	13574	Dune	61.90	38.10	0.00
80	13653	Apron	41.18	52.94	5.88

Sandstone Architecture and Framework Grain Composition

The Nugget Sandstone architecture in this study is 88% framework grains, 9% matrix, and 3% cement ($F_{88}M_9C_3$ - Fig. 22). The thin-section microscopy reveals that the main mineral component of all thin sections of sandstones is represented by quartz grains, which are associated with potassium feldspar (predominantly orthoclase), and minor amounts of lithics (mainly chert). The framework grain composition is by and large subarkosic with 87% quartz, 13% feldspar, and 2% lithics as plotted on a QFL diagram. ($Q_{87}F_{13}L_2$ - Fig. 23). Several samples are mature sandstone classified as quartzarenites.

Framework Grains

By far monocrystalline quartz is the main grain type: well 30-02 (70-91%), well 16-20 (70-94%), and well 29-04ST1 (44-91%). Sample 29-04ST1-16 is a very immature sandstone with 41% potassium feldspar. The average amount of monocrystalline quartz is

Table 6. Percentages of pore-filling material from well 20-16

Sample	Depth (ft)	Facies	Kaolinite	Illite	Cataclasite	Oil	Nimite
15	11874	Apron	100.00	33.33	0.00	0.00	0.00
19	11946	Apron	0.00	16.67	0.00	100.00	0.00
20B	11972	Apron	43.48	56.52	0.00	0.00	0.00
22	11992	Apron	0.00	45.45	0.00	100.00	0.00
26	12063	Apron	0.00	0.00	0.00	0.00	0.00
30	12116	Dune	0.00	3.33	0.00	100.00	0.00
33	12146	Dune	33.33	66.67	0.00	0.00	0.00
34	12147	Dune	22.22	44.44	11.11	11.11	11.11
41	12222	Apron	0.00	0.00	0.00	75.00	25
43	12341	Dune	0.00	0.00	0.00	100.00	0.00
44	12351	Apron	16.67	0.00	0.00	50.00	33.33
46	12432	Dune	0.00	0.00	0.00	100.00	0.00
48B	12468	Interdune (Dry)	0.00	14.71	0.00	100.00	0.00
50A	12500	Apron	0.00	0.00	0.00	0.00	100.00
59A	12710	Interdune (Wet)	25.00	0.00	0.00	0.00	75
61A	12742	Interdune (Wet)	100.00	57.14	0.00	0.00	0.00
51B	12811	Apron	0.00	0.00	0.00	0.00	0.00
54B	12857	Interdune (Wet)	50.00	50.00	0.00	0.00	0.00
53B	12872	Dune	66.67	0.00	0.00	0.00	33.33
57	12903	Interdune (Wet)	0.00	0.00	0.00	0.00	0.00
63B	12979	Apron	100.00	0.00	0.00	0.00	0.00
1	13050	Apron	0.00	0.00	0.00	0.00	0.00
28B	13067	Interdune (Wet)	0.00	0.00	0.00	0.00	0.00
2	13073	Apron	0.00	0.00	0.00	0.00	100.00
5	13125	Interdune (Wet)	0.00	0.00	0.00	0.00	100.00
8	13186	Interdune (Dry)	0.00	0.00	61.11	38.89	0.00
12	13244	Interdune (Wet)	0.00	100.00	0.00	0.00	0.00
74	13521	Apron	0.00	0.00	76.47	0.00	23.53
75	13527	Apron	0.00	0.00	35.29	17.65	47.06
77	13574	Dune	0.00	0.00	0.00	50.00	50.00
80	13653	Apron	0.00	0.00	75.00	25.00	0.00

76% for all of the samples that were point counted. Polycrystalline quartz is not volumetrically significant, averaging about 2% of the framework grain fraction. Quartz grains appear to be highly stained in well 16-20 near the hinge of the anticlinal structure that makes up Anschutz Ranch East field.

Feldspar grains are overwhelmingly potassic in composition, with scarce to absent plagioclase grains making up the framework. Both orthoclase and microcline are present, but orthoclase is the main feldspar grain. Potassium feldspar is the only other significant framework grain and it only accounts for an average of 10%, but does have a variable range between wells: 30-02 (3-19%), 16-20 (1-23%), and 29-04ST1 (5-40%).

Feldspar grains that have altered partially or almost entirely to kaolinite are found

Table 7. Percentages of framework grains from well 29-04ST1

Sample	Depth (ft)	Facies	Qm	Qp	K-spar	Plag	Alt K-spar	Ls	Lm	Lv	Lp	Zeolite
1	12073	Apron	80.59	1.47	12.82	0.00	2.56	1.83	0.00	0.00	0.37	0.37
3	12145	Apron	90.60	1.88	5.26	0.00	1.88	0.38	0.00	0.00	0.00	0.00
5	12174	Apron	74.62	6.92	15.00	0.38	0.77	1.15	0.00	0.38	0.00	0.77
8	12207	Dune	86.06	3.83	7.32	0.00	1.39	1.05	0.00	0.00	0.35	0.00
11	12660	Apron	76.61	7.26	11.69	0.00	0.40	1.61	0.40	0.00	0.81	1.21
12	12663	Dune	74.53	4.12	14.23	0.00	3.00	1.12	0.00	0.00	0.75	2.25
14	12689	Apron	72.43	4.12	20.58	0.82	1.23	0.82	0.00	0.00	0.00	0.00
15	12699	Apron	78.91	4.30	14.06	0.00	0.78	0.78	0.00	0.39	0.39	0.39
16	12719	Apron	44.07	5.08	40.68	0.00	1.69	0.00	0.00	0.00	8.47	0.00

Table 8. Percentages of cement from well 29-04ST1

Sample	Depth (ft)	Facies	Carbonate	Quartz	Hematite
1	12073	Apron	55.56	22.22	22.22
3	12145	Apron	60.00	20.00	20.00
5	12174	Apron	72.73	13.64	13.64
8	12207	Dune	100.00	0.00	0.00
11	12660	Apron	29.41	35.29	35.29
12	12663	Dune	6.25	46.88	46.88
14	12689	Apron	40.43	29.79	29.79
15	12699	Apron	57.14	21.43	21.43
16	12719	Apron	33.33	33.33	33.33

Table 9. Percentages of pore space fill from well 29-04ST1

Sample	Depth (ft)	Facies	Kaolinite	Illite	Cataclasite	Oil	Nimite
1	12073	Apron	0.00	100.00	0.00	0.00	0.00
3	12145	Apron	43.48	52.17	0.00	0.00	4.35
5	12174	Apron	11.11	33.33	0.00	11.11	44.44
8	12207	Dune	22.22	33.33	0.00	33.33	11.11
11	12660	Apron	33.33	66.67	0.00	0.00	0.00
12	12663	Dune	45.45	54.55	0.00	0.00	0.00
14	12689	Apron	14.29	7.14	78.57	0.00	0.00
15	12699	Apron	8.33	8.33	41.67	8.33	33.33
16	12719	Apron	25.00	25.00	0.00	50.00	0.00

throughout the Nugget Sandstone, but percentages are low. Altered feldspar grains were also point counted separately from unaltered feldspar grains, which allowed for a better understanding of the diagenetic history of the Nugget Sandstone in Anschutz Ranch East field. Altered feldspar grains only account for 1% of the average total rock volume, but there is some variability within wells: 30-02 (0-2%), 16-20 (0-5%), 29-04ST1 (0-3%). The high percentage of potassium feldspar suggests a volcaniclastic source.

Lithics are very scarce and have an overall average of 1% total rock volume with little variation between the wells: 30-02 (0-3%; average 1%), 16-20 (0-3%; average 1.5%), and 29-04ST1 (0.6-3%; average 1.9%). The more common varieties of lithics include:

Table 10. Statistics of porosity values well 30-02 separated out by facies

Dune Facies		Apron Facies	
Mean	10.46132	Mean	8.40037
Standard Error	0.130232	Standard Error	0.188839
Median	10.8	Median	8.2
Mode	12	Mode	7
Standard Deviation	2.488084	Standard Deviation	3.102949
Sample Variance	6.190561	Sample Variance	9.62829
Kurtosis	-0.54132	Kurtosis	-0.27115
Skewness	-0.27904	Skewness	-0.19273
Range	14.72	Range	14.4
Minimum	1.48	Minimum	0.5
Maximum	16.2	Maximum	14.9
Sum	3818.38	Sum	2268.1
Count	365	Count	270
Largest(1)	16.2	Largest(1)	14.9
Smallest(1)	1.48	Smallest(1)	0.5
Confidence Level (95.0%)	0.256102	Confidence Level (95.0%)	0.371791

Dry Interdune Facies		Wet Interdune Facies	
Mean	6.460357	Mean	6.967836
Standard Error	0.150786	Standard Error	0.122772
Median	6.7	Median	7.1
Mode	7.1	Mode	7.4
Standard Deviation	1.784122	Standard Deviation	1.605456
Sample Variance	3.183093	Sample Variance	2.577489
Kurtosis	2.908032	Kurtosis	0.69049
Skewness	-1.14204	Skewness	-0.21444
Range	9.69	Range	9.5
Minimum	0.01	Minimum	2.1
Maximum	9.7	Maximum	11.6
Sum	904.45	Sum	1191.5
Count	140	Count	171
Largest(1)	9.7	Largest(1)	11.6
Smallest(1)	0.01	Smallest(1)	2.1
Confidence Level (95.0%)	0.29813	Confidence Level (95.0%)	0.242355

chert, quartz rich schist, felsic volcanic clasts, and plutonic clasts (mica).

Matrix

Matrix is present as very scarce amounts of pore filling material, more frequently as coats around grains. The matrix in the sandstone averages 9%, although it commonly constitutes less than 1%. The majority of the matrix is authigenic and not detrital, which would be expected because of the complex diagenetic history discussed later. Also, as the total rock volume of matrix increases, there is a reduction in the suturing of grains and authigenic overgrowths. Details of the mineralogy in the rocks were determined by X-ray diffraction methods. A sample of an XRD analyses (Fig. 24) shows the nature of the results from this study. Minor constituents can be differentiated using XRD, as described below.

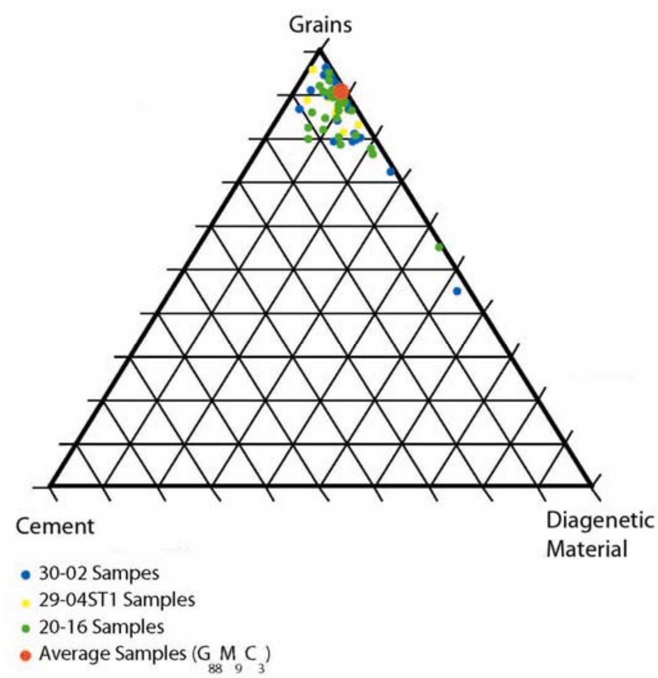

Figure 22. Nugget sandstone composition based on point counts of 58 thin sections.

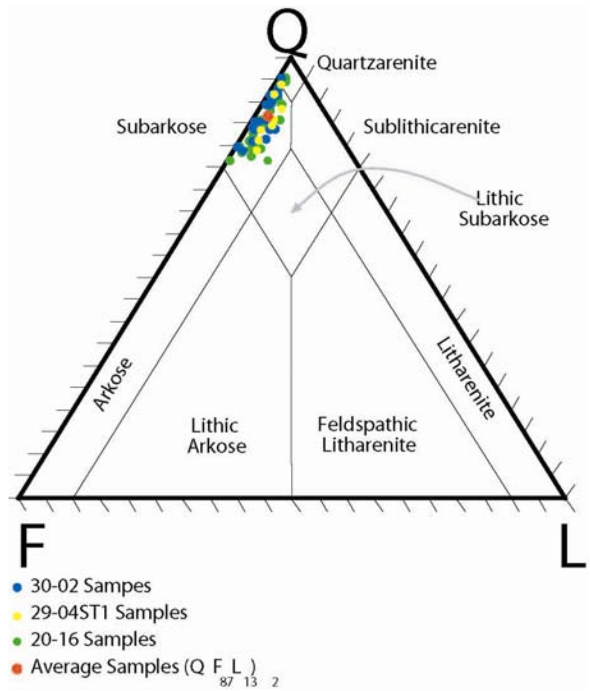

Figure 23. Nugget Formation QFL diagram showing the composition of 58 sandstone thin sections. Classification triangle is modified after McBride (1963). Petragraphic analysis was conducted by modifying the Gazzi-Dickinson point counting method; see text for explanation.

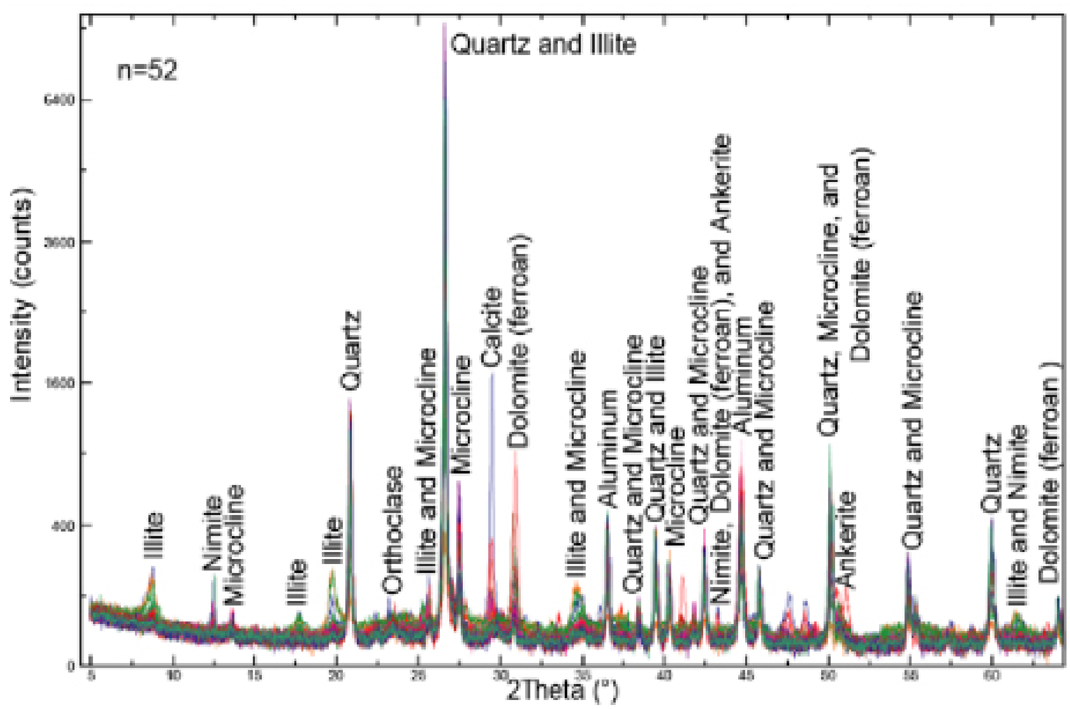

Figure 24. Determination of bulk composition of the Nugget Sandstone by x-ray diffraction (XRD). XRD results indicate the microcline is the dominant feldspar. XRD analysis also indicates that ferrodolomite is the chief carbonate cement.

Pore-Filling Material

Bitumen

The presence of bitumen (dead oil) (Fig. 19) in pores indicates that hydrocarbons were once producible from the Nugget Sandstone but were altered by some geochemical process, leaving an insoluble residue. A minor amount of bitumen has been found in thin section (0-10%, average 0.8%). When considering the amount of bitumen that is pore filler in each of the wells the distribution is quite variable: 30-02 (0-100%), 16-20 (0-100%), and 29-04ST1 (0-50%). Bitumen can be very effective at filling pore space but it is more commonly seen where it leaves the pore space void and bridges the pore throat. In thin section, bitumen is an amorphous, brownish black solid. As discussed later, oil post dates the structural deformation of Anschutz Ranch East field.

Anschutz Ranch East field contains a rich retrograde gas-condensate with a dew point slightly below the virgin reservoir conditions, meaning that the condensate was in the gas phase under original reservoir pressure conditions. Once the pressure was dropped in the field the condensate reached critical point and entered the liquid phase and consequently a loss of reserves in place occurred (Kleinsteiber et al., 1983). Where bitumen is seen it serves as a first guide to relatively high reservoir quality that was degraded during production.

Clay Minerals

Kaolinite is common and appears as a thin transparent tan film on detrital feldspar grains that have been altered. In this study, kaolinite was only counted when the clay mineral was taking up pore space and wasn't counted when it appeared as a thin film on altered feldspar grains. Altered feldspar grains were counted separately. The total rock volume for kaolinite is very small (0-3%, average 0.3%). When considering the amount of kaolinite that is pore filler in each of the wells the distribution is variable: 30-02 (0-11%), 16-20 (0-100%), and 29-04ST1 (0-45%).

Authigenic illite is slightly more common than kaolinite (0-4%, average 0.6%). When considering the amount of illite that is pore filler in each of the wells the distribution is quite variable: 30-02 (0-43%), 16-20 (0-100%), and 29-04ST1 (0-45%). Net (2003) determined that smectite clays were converted to illite with increased burial depth and temperatures related to tectonism in Anschutz Ranch East field. Clay minerals are scarce to absent and do not significantly reduce the porosity. However, there is a clear negative correlation of porosity with respect to the degree of quartz cementation.

Authigenic Feldspar

Authigenic potassium feldspar is not common but it is seen periodically throughout most of the thin sections that were analyzed. When feldspar overgrowths are seen, they develop a euhedral crystal shape on detrital feldspar grains. Usually the detrital grains are sufficiently altered, so that the rounded detrital feldspar is in marked contrast with the clear, unaltered authigenic feldspar. A film of iron oxide or kaolinite coating often marks the contact of the two feldspars. The rounded shapes of detrital grains indicate a comparatively long sedimentary history before their deposition, which suggests that growths are authigenic. Feldspar overgrowths develop prior to carbonate concretions, thus, authigenic feldspar had to develop very early in the diagenesis of the Nugget Sandstone.

Nimite

Sporadically, an apple green to yellowish-green mineral occurs in both deformed and undeformed rock. The cement-like mineral is nimite, which is a clay mineral in the chlorite group. When nimite occurs in undeformed rock, it seems to preferentially be distributed in porous and highly permeable beds. The nimite occurs as a minor pore-filling grain and on slip surfaces of faults. Nimite is probably the result of an in-situ alteration of unstable detritus in the host rock.

Chlorite does not occur often but comprises up to 10% of some samples (sample #16-20-26). Nimite on average only comprises 0.5% of the total rock volume, but varies between wells: 30-02 (0-1.3%; average 0.7%), 16-20 (0-2.6%; average 0.4%), 29-04ST1 (0-1.3%; average 0.4%). Nimite typically has a radial morphology with rosette-like structure in high porosity and permeability beds. Within fine-grained beds, nimite has a ratty sheet-like morphology.

Cements

The main cement encountered in this study includes calcite, dolomite, and quartz. Minor hematite makes up small percentages of the total cement.

Carbonate Cement

Carbonate cements show an extremely variable distribution in total rock volume (from 0-36%, average 5.4%), which is also reflected in the fabric. Carbonate cement is common. Net (2003) suggests that ferroan dolomite is the most common agent in the Nugget Sandstone. However, in this study the thin sections were not stained for carbonate, which makes it difficult to determine whether the cement is calcite or dolomite. Dolomite was counted when distinct rhombs were seen.

The upper two zones of the Nugget are dominantly cemented with carbonate (Plate 3) with small disruptions of quartz cement. There are small variations in the total cement weight percentage of carbonate: well 30-02 (0-98%), well 16-20 (20-100%), and well 29-04ST1 (6-100%).

Carbonate cement has both microcrystalline and poikilotopic textural characters, which are distinctly different and possibly related to climate and/or weathering prior to burial. Poikilotopic cement is very common in the dune facies where carbonate cement takes on a pervasive nature in coarse-grained beds, possibly due to the high permeability avalanche deposits. Just as pervasive cementation is common within the dune facies, carbonate concretions are also common. These concretions are probably the precursor of pervasive cementation, because both have uniformity in the extinction of twinning. Microcrystalline cementation is more frequent where dissolution has occurred and intense quartz overgrowths are present.

Quartz

Quartz cement accounts for a very small fraction of total rock volume (0-6%, average 1.6%) and shows a very wide range in the cement weight percentage: well 30-02 (0-71%), well 16-20 (0-53%), and well 29-04ST1 (0-46%). These variations in the cement weight percentage of quartz are possibly linked to diagenetic temperatures, burial depths, and tectonic locations. Overall quartz cement is most prevalent within zone 3 (Plate 3).

Petrographic observations indicate that quartz cement probably began to grow as individual, tiny pyramidal crystals along the surface of detrital grains. These tiny crystals are common where there isn't any evidence of pressure solution. Also, there are occasionally tiny quartz crystals within carbonate concretions, however they are not common.

The boundary between detrital quartz grains and tiny overgrowths is clearly visible and form in continuity with the underlying quartz grain. Under high magnification these boundaries are visible by the abundance of inclusions trapped between the overgrowths and the grain. In areas where overgrowths form larger euhedral crystals, pressure solution seams are widespread. At this advanced stage of overgrowth cementation, boundaries between detrital grains and overgrowths are weakly visible. The contacts between adjacent overgrowth boundaries are irregular and produce a mutual interference during crystal growth. Where the correct diagenetic conditions were met, these tiny quartz overgrowths would merge later into large interlocking, euhedral overgrowths.

Hematite

Coating of grains with hematite is the earliest recognizable cementation event that occurred, which is very useful in delineating original grain boundaries. In thin section, well-developed hematite crystals occur as very small platelets that are deep red-brown color, but typically crystals are rather small and opaque.

Variable amounts of hematite occur in thin section (0-32%, average 2.1%). Hematite cement weight percentages range for each well are: 30-02 (0-62%), 16-20 (0-68%), and 29-04ST1 (0-46%). Hematite isn't as prevalent as carbonate and quartz cement. However, it still is a considerable factor in the cementation of the Nugget Sandstone. It appears as a thin coat along many of the grains. Where hematite is present, it is fine grained with an irregular distribution, occurs in thick zones, and lies in discontinuities along grains. Net (2003) observed that there was no evidence of hematite crystals under SEM, which lead to the suggestion that former infiltrated clays may have acted as the source for iron. The hematite may be primary in their origin; that is, many grains may have been coated at the time of deposition or at least early on in the Nugget's diagenesis.

Hematite is the most the common cement within the lower portion of the Nugget (zone 3), in areas of Anschutz Ranch East field where extensive amounts of fluid flow probably hasn't occurred. This may be due to chemical reduction and subsequent removal by reaction with the organic matter in the oil.

Thin and discontinuous coatings of hematite cement do not impede quartz overgrowth development because there is very commonly a hematite ring coating grains under quartz overgrowths. Locally thick and/ or continuous coats around grains will retard the growth of authigenic quartz.

Geochemical analyses of cements

The abundance of carbonate cement ("snow flakes") and hydrocarbon staining (zebra banding) in porous beds allowed us to determine the volumetric abundances of carbonate cement and bitumen in the pores of the Nugget Sandstone in Anschutz Ranch East field. Several techniques were used in the analysis of the five samples examined - two from well 30-02; three from 16-20.

Well 30-02

Carbonate-Rich Horizon

A limey siltstone from the wet interdune facies in well 30-02 sampled at 13,330 ft (4066 m) contains 47% carbonate cement of the total rock volume. Such a high percentage of carbonate cement suggests that this interval was a small lake or pond. The sample also contains ~8% of total organic carbon (TOC) which may represent a lake or pond that was long lived to develop such a high value. Carbonate-rich horizons in eolian depositional environments are usually considered to be freshwater deposits that accumulate in ponds in the interdune area (Ahlbrandt and Fryberger, 1981; Eisnberg, 2003; Net, 2003).

Oxidized Mudstone

An oxidized mudstone from wet interdune facies in well 30-02 was sampled [sample #30-02-100; at 14,124 ft (4307.8 m)] and contains 21% carbonate cement. Such a high percentage of carbonate cement suggests that this interval represents a small lake or pond. The sample also contains ~2% TOC.

Well 16-20

Carbonate Concretions

Throughout much of the dune and apron facies carbonate concretions are prevalent, which record an early diagenetic event. A sample from the apron facies in well 16-20 [sample #16-20-20B; at 11,972 ft (3651.5 m)] has only 6% carbonate of the total rock volume. This value was much lower than expected, which means porosity is affected by this diagenetic event but not to the extent that might have been expected based on a visual inspection of the core. Hydrocarbon staining is likewise deceptive, with only 0.1% TOC value in the sample. Thus, this would suggest that the carbonate concretions do affect the reservoir by lowering the permeability, but do not have much of an influence on the overall porosity of the rock.

Carbonate-Rich Zones

Periodically pervasive carbonate cementation occurs in much of the dune and apron facies. Sample #16-20-28B [13,067 ft (3985.4 m)] was taken from apron facies, where an entire bed has intense carbonate cementation. In thin section, carbonate cement appears to take up all of the pore space in the sandstone. Carbonate accounts for 38% of the total rock volume. Intense cementation occurring along a single bed will cause anisotropy in a reservoir.

Bitumen-Rich Sandstone

Well 16-20 has an interval [12,115 ft (3695 m)] of sandstone within a dune facies section that appeared to be tar sand. The sandstone was very porous and smelled of hydrocarbons. This interval (sample #16-20-30) has 0.8% carbonate and 1.7% of bitumen. In thin section, the pore throats were bridged with bitumen and the pore space was void. This is not critical in the investigation of the study. It was evaluated to better characterize the Nugget Sandstone in Anschutz Ranch East field.

DEFORMATIONAL CHARACTERISTICS

Fractures

Fractures are common elements throughout the core, and consist of open fractures, closed fractures, deformation bands, and fractures filled with secondary mineralization.

Closed Fractures

Typically fractures are filled with cryptocrystalline silica cement, and XRD analyses indicates that in many cases the silica cement is low quartz. This filling is most common in the lower 357 ft (108.81 m) of well 30-02. This suggests that elevated temperatures and pressures promoted fracture healing and cementation with the quartz.

Deformation Bands

In thin section, deformation bands show a different texture from the host rock. In nearly all instances, strain shadows extend from the original grain to the overgrowth, suggesting that straining is indeed post-deposition and not a feature of the quartz grain prior to sedimentation. Single deformation bands show brittle deformation in grain size, which probably results in a reduction in porosity. At band margins, and throughout single bands, grains are prominently fractured and crushed, with production of highly angular grain fragments. As grain size increases, there appears to be a decrease in the amount of strain that was exerted on the grains.

Deformation bands are recognized by well-developed, continuous zones of grain size and porosity reduction and are bounded on both sides by compacted grains. Porosity reduction begins by the collapsing of the pore space and was later accompanied by the rotation and translation of rigid grains. In contrast, within the well-developed shear zones of several bands, intergranular fracturing is not significant. Instead, within these interior portions of shear zones, there are comparatively small numbers of large and rounded grains. The grains present are quartz that show dextral shear and have an s-fabric. The core of shear zones is made up almost entirely of sub-micron size cataclasite cement. Porosity is dramatically decreased, if not completely absent in these zones.

In contrast to single bands, well-developed shear zones have a main discrete slip-surface. Along the main slip-surface in the core of a shear zone precipitation generally has not occurred. However, within the core of a shear zone there are several slip-surfaces with translated quartz grains. All of the observations show deformation bands evolving from the host rock to deformation bands without cataclasite, to well-developed shear zones with cataclasite and several slip-surfaces. Where present, potassium feldspar grains generally make up the bulk of grain composition within the deformation bands. Deformation bands are most commonly developed in the dune facies and these bands clearly compartmentalize the location of oil in some parts of the reservoir.

INTERPRETATIONS

Stratigraphy of the Nugget Sandstone in Anschutz Ranch East Field

Core from the vertical well 30-02 represents a complete section for the Nugget Sandstone in Anschutz Ranch East field. In published literature the Nugget is commonly divided into three zones, with zone 3 as the basal unit. Generally these divisions are described as stratigraphic sequences, but are inferred from petrophysics.

The lower 15 ft (4.6 m) of core is comprised of reddish siltstone with sub-vertical burrows, which matches Chan's (1999) description of the upper member of the Ankareh Formation. That siltstone is overlain by zone 3 of the Nugget, which begins with a thick secession (~140 ft; 42.7 m) of reddish-brown, moderately sorted, very fine- to fine-grained sandstone beds with the occasional thin, silty-mud drape. Sand-size grains comprise most of this package of rock with a significant portion of the pore space occupied by clay-size grains. Authigenic clays and detrital grains are chiefly responsible for clogging pore throats.

Lithologically, the lower 140 ft (42.7 m) of zone 3 is characterized by thin horizontal beds with high-amplitude ripples, burrows, and soft-sediment deformation with the occasional scoured bedding surface. Several intervals also consist of convoluted beds. In order for high-amplitude ripples to form the sediment must have had some cohesion (Fryberger et al., 1979). The interpretation that this sequence was saturated is supported by the presence of convoluted beds and soft-sediment deformation. In addition, given the lack of any root casts, paleo-soils, or organic rich beds, the region was most likely poorly vegetated.

The sand grains have a frosted texture, which is very common for sediment in eolian systems (Net, 2003). Even though the newly deposited sediment was transported by wind, lithological evidence points to a semi-arid climate with a periodic influence by subaqueous processes. Evidence such as the thickness of this package of rock supports the idea that the entire region had a similar moistening environment. Sediment was probably moistened by wicking moisture from a high water table, which is often the case in a wet eolian system (Kocurek and Havholm, 1993). Moisture is also the likely explanation for the presence of detrital clay in pores. Moisture would have allowed for cohesion of the sediment and prohibited the clay from being swept away by wind.

Lithology, sedimentary structures, and grain texture indicate that the lower portion of zone 3 was probably a wet interdune facies in what was a sabkha environment (Fryberger et al., 1979). Additional evidence that support a sabkha depo-system includes the fact that the XRD analysis shows the presence of evaporites and there is no evidence of remnants of vegetation in the rock. Furthermore, carbonate cements in this interval of core are dolomitized, signifying perhaps the presence of a vadose zone (Badiozamani, 1973).

Shortly after deposition, we interpret the lower portion of zone 3 to have experienced an increase of cohesion, perhaps caused by wicking of water from a high water table. With the high rate of evaporation that commonly takes place in sabkha depo-systems (Fryberger et al., 1979), moisture within the sediment would have quickly evaporated. Thus, this 140 ft (42.7 m) of core represents an eolian dune system that built out onto a low-lying coastal plain, much like the Arabian Gulf coastline near Dhahran, Saudi Arabia (Fryberger et al., 1979).

The upper portion of zone 3 (~180 ft; 54.9 m) is predominantly a reddish-brown, very fine to fine-grained sandstone. Lithologically the upper portion of zone 3 consists of inversely graded, low-amplitude ripples; as well as thin horizontal beds similar to those described by McKee and Tibbets (1964), Fryberger et al. (1979), Ahlbrandt and Fryberger (1981), and Kocurek, (1981). Low-amplitude, inverse-graded ripples are indications of downwind climbing translated strata formed by translation of wind-ripples under enough sand supply (Hunter, 1977; Kocurek, 1981). Lack of adhesive sedimentary structures indicates that the sediment was rarely damp. In addition, sparse mud indicates that flooding likely didn't frequently occur. The presence of abundant wind-ripples suggests a semi-arid depo-system. The sedimentary sequence consists of moderately sorted, fine-grained texture, which implies that deposition occurred above the water table and capillary fringe level. Thus, the upper portion of zone 3 is interpreted to have a dry interdune facies and deposition occurred within a sand sheet.

Even though the sediment is moderately sorted, there isn't the unique bimodal distribution (pin-stripes) of grain size characteristic of eolian dune slip-faces. There are occasional intervals of rock that are on the scale of 15-20 ft (4.6-6.1 m) that do contain "pin-stripe" laminae, but these are minor when considering the entire upper package of zone. These intervals of core that contain occasional "pin-stripe" laminae are commonly considered to be characteristic of eolian dunes (Brookfield, 1977; Hunter, 1977; Lancaster, 1981), but are conceivably small eolian dunes that marched across a low-lying sand sheet.

Hummel and Kocurek (1984) suggest that thick dry interdune deposits are uncommon in the rock record because the sediment tends to be swept away. This suggests two ideas: 1) a positive sediment budget, and 2) a large amount of accommodation space. Consequently, there would be little scope for erosion and only accumulation of sediment would have occurred. Thus, there would be little to no time for fine material to be swept away.

Zone 3 of well 30-02 is overlain by a thick package (485 ft; 148 m) of buff to red, well-sorted, very fine to medium sandstone. Nearly all of the grains are well rounded to sub-angular and have a frosted texture, which suggests sediment transport by wind (McKee and Tibbets, 1964). However, sedimentary structures such as inversely graded, high-amplitude ripples suggest that deposition occurred by wind and not by a subaqueous process. In the core examined in this study, the most indicative sedimentary structure that suggests eolian deposition is "pin-stripes," which is very common in the two main types of facies within zone 2. Also the absence of marine deposits such as clay drapes, fossils, and/or traces fossils suggest an eolian process. The thickness of zone 2 indicates eolian deposition in a very large system such as an erg, rather than merely coastal dunes. The absence of clay drapes suggests that there was no tidal influence. Overwhelmingly zone 2 indicates an increase in the aridity of the region and possibly sediment supply.

High resolution of what in the lithologic logs indicates considerable heterogeneity within zone 2, rather than a single, continuous interval of eolian sand with only dune facies. The two main facies that are present in zone 2 are expressed in alternating packages of rock with dune and apron facies. The dune facies range in thickness from 25-85 ft (7.6-25.9 m), while the apron facies range from 20-50 ft (6.1-15.2 m). The occurrence of dune facies indicates the migration of eolian sand and the greater development of an erg. The thickness of intervals of rock with dune facies doesn't have any connection in direct height of a dune because the core was not examined for bounding surfaces that Brookfield (1977) described. Thickness of these intervals only suggests that deposition occurred along the lee side of a dune and there may have been several small dunes migrating over each other. Lack of large-scale cross-stratification in Nugget Sandstone outcrops also suggests smaller scale dunes than are present in the Navajo Sandstone.

The apron facies suggests a stagnant period of the erg system. Alternating intervals of dune and apron facies in zone 2 suggests that there were periods of greater deposition than others. These periods of greater deposition have been interpreted as several consecutive moderate sized eolian dunes migrating over each other, rather than being a single, large migrating dune front.

In well 20-16, there are two intervals that have a distinctly dry interdune facies and not just an apron facies, mainly because the overall thickness of these intervals is 34-38 ft (10-12 m). Thick intervals that are characterized by horizontal beds and high amplitude ripples suggest a sand sheet deposystem. In order for a change in deposition to occur between well 30-02 and 20-16 there must have been considerable lateral variations in the erg system, because the distance between the two wells is approximately one township (6 miles [9.7 km]). These variations in well 20-16 suggest that the Jurassic sand sea was not simply a straight transverse dune system, but probably had a barchan dune component. This would be very comparable to the modern sand sea of the Sahara Desert in Libya.

Two thin (2-3 ft; 0.6-0.9 m) intervals of rock are characterized as having soft-sediment deformation, such as slumping, and have been interpreted as having a wet interdune facies. McKee (1971) points out that wet sand (i.e., sand that is uniformly wetted but not saturated) has the highest values of cohesion. It is likely that the presence of soft-sediment deformation indicates a wetter period of time. This local change to subaqueous deposition may have been the result of an ephemeral stream that wetted the sand and allowed for soft-sediment deformation. Because of the topography involved in eolian systems, an ephemeral stream presumably flowed along interdune corridors, much like the Hoanib River in Namibia, which flows a few days a year in the dune field, enabling soft-sediment deformation in interdunal depressions (Stanistreet and Stollhofen, 2002).

In well 30-02, zone 1 is 215 ft (65.5 m) thick and is characterized by dune and apron facies, similar to zone 2. However, at the base of zone 1 there is an interval of rock (seen in both well 30-02 and 20-16) that differentiates zone 1 and 2. This interval in well 30-02 is only 3 ft (0.9 m) thick, and is a carbonate-rich siltstone with a high TOC value. The TOC is most likely the result of algae forming in a body of water with very little water circulation (LeTourneau and Hiber, 2006). The XRD analysis of this interval indicates no presence of evaporites, which suggests fresh water instead of marine (Ahlbrandt and Fryberger, 1981; LeTourneau and Hiber, 2006). These data suggest the sediments were deposited in an interdunal pond, which would have allowed for carbonate precipitation and algae growth. This suggests that there was more than periodic ephemeral wetting events, and instead a regional climate change may have raised the water table.

The basal 27 ft (8.2 m) of zone 1 in well 20-16 is also described as having a wet interdune facies. However, this interval in well 20-16 is not rich in carbonate, but is extensively bioturbated. In order for the sediment to be extensively bioturbated, water had to be present for life to occur.

Drastic changes in depositional style such as that described above are typically interpreted as a super-bounding surface. This would imply a hiatus in deposition or dunes migrating through without net accumulation of an erg (Chan et al., 1992). Since this wet interdune facies occurs in both wells, a climate change is the most realistic explanation, which would spawn a hiatus in eolian deposition. The depositional hiatus would be caused by the sediment becoming damp and/or wet, generating cohesion in the sediment and not allowing sediment to be transported by wind.

As for the dune and apron facies in both of the wells, there is a considerable amount of variability. Well 30-02 has a thick interval of rock with dune facies, while well 20-16 is overall characterized by apron facies, suggesting once again that the erg system was migrating at different rates in these two locations.

Well 30-02 displays the contact between the Nugget and Twin Creek formations, which places marine deposits on top of eolian deposits and indicates the presence of a major flooding surface. This flooding surface marks the termination of eolian deposition as well as indicating when the Sundance Sea flooded the North American craton.

In summary, we propose a conceptual model (Fig. 25) for deposition of the Nugget Sandstone in Anschutz Ranch East field that began with eolian system building out on to a low-lying coastal plain where a sabkha depo-system formed. The sabkha depo-system would have been at least partially saturated and possibly influenced by sea water mixing with ground water. With further migration of the eolian system, topographic relief would have increased and deposits influenced by the presence of the water table would have given way to a high sediment supply regime. Thus, the sabkha and sand sheet depo-systems represent the fore-erg of the greater Jurassic sand sea as it migrated southward.

Following the migration of the fore-erg, the development of eolian dunes would have occurred, assuming there was an abundance of sediment for transport and the capacity of the wind was sufficient to move that material. As a consequence, sedimentation and deposition would have occurred, whereby, dune growth would have been promoted and over time a dune field would have developed. Bergosh et al., (1982) suggests morphology of transverse dunes based on outcrop and borehole data. In addition, McKee and Bigarrella (1979) suggested that the Jurassic sand sea was a compound dune field consisting of many superimposed dunes of similar morphology. A modern analog for this depo-system would appear much like the Sahara of North Africa.

A climate change would have also resulted in the shut-down of erg migration and possibly would have resulted in erosion. Since there was no evidence of a deflation surface such as desert pavement in any of the core analyzed in this study, the development of

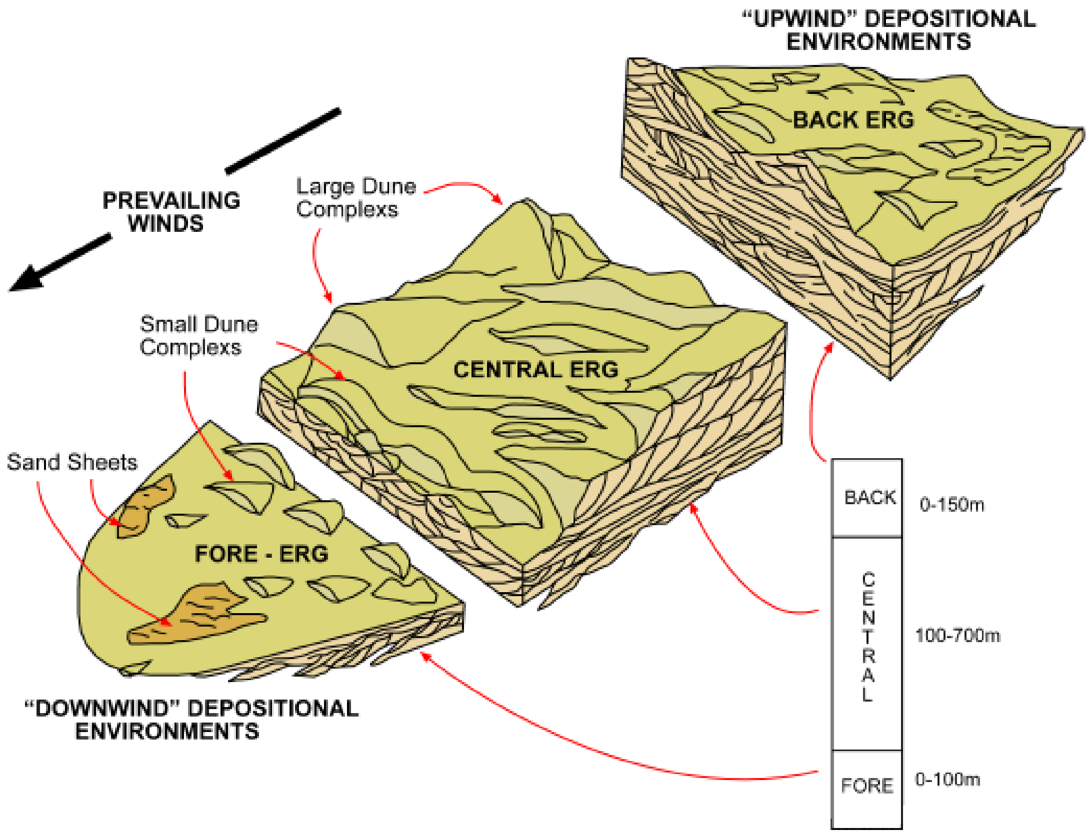

Figure 25. Eolian depositional block diagram illustrating the migration of an erg system with an idealized vertical stratigraphic sequence of a: fore-erg, central-erg, and back-erg. The divisions are based on types and scale of eolian strata and the nature of intra- and extradunal facies. Modified from Morse (1994). The fore-erg would represent Zone 3 of the Nugget Sandstone, while the central-erg most likely represents Zone 2. It is possible that Zone 1 can be represented by the upper portion of the central-erg or the back-erg.

erosion on a large scale is inferred to not have occurred. However, the development of an interdunal pond with carbonate precipitation and algae growth in well 30-02 and evidence of subaqueous deposition in well 20-16 suggests a brief shut-down of erg migration caused by a climate change. This shut-down of the erg migration may be a signal that global atmospheric conditions were about to change. An important shift from arid and terrestrial to humid and marine conditions did occur with the deposition of the Twin Creek Limestone.

Diagenetic Chronology

The principal parameters that were investigated in core for a diagenetic affect are: framework constituents, texture, intergranular cements, matrix, and hydraulic conductivity. These parameters are essentially a function of depositional environments (facies), fluctuating ground-water chemistry, and post-depositional environments.

The Nugget Sandstone was deposited principally in an eolian environment. Shortly after deposition, weathering of detrital grains occurred by chemical alteration. Minerals such as potassium feldspar and clay minerals are affected by low temperature (-20 to 50^{o}C), low pressure (near surface pressures), and free oxygen (P. Kolesar, oral comm., 2006).

The formation of smecitite from potassium feldspar through weathering was a very significant early diagenetic event in Anschutz Ranch East field (Net, 2003).

Smectite is very commonly seen near weathered potassium feldspar grains in thin section. Net (2003) determined that there is a regional distribution of authigenic clay (mainly smectite) in the Nugget and Navajo formations that experienced relatively low burial temperatures. Net (2003) also determined that the Nugget Sandstone in Anschutz Ranch East field experienced more intense temperatures and/or burial depth. The increase in temperature is what most likely caused the smectite-illite reactions to occur. This would explain why illite is the dominate clay mineral seen in the XRD analysis.

The suggestion of smectite forming early is supported by the abundance of authigenic hematite. Thin and discontinuous coats of hematite cement occur on nearly all of the detrital grains when viewed in thin section. In intervals of core, hematite has more intense hues, and is typically seen within both wet and dry interdune facies. McBride et al. (1987) suggests that hematite is mostly derived from the early alteration of clays. This would explain the red to buff tint that is common to the Nugget Sandstone, however there is a stark contrast where bleaching occurred by the migration of hydrocarbons. The contrast between bleached and unbleached rock is clear when comparing well 30-02 (unbleached) and 20-16 (bleached) (Plate 3).

Shortly after deposition, but after the formation of hematite coating grains, early mechanical compaction took place. Mechanical compaction occurred though the rearrangement of framework grains and grains moving closer together. Rearrangement of framework grains occurs by the physical processes of rotating and slipping of grains, plus the ductile bending of weak grains such as mica. In quartz-rich sandstones, such as the Nugget Sandstone, that lack ductile grains (shale fragments), grain slippage is the chief mechanism of compaction (Füchtbauer, 1967). Paxton et al. (2002) suggests that in rigid sand grains such as the ones in this study, porosity can be reduced with progressive burial from depositional value of 37-40% to less than 20% (Schenk, 1983; Dickinson and Ward, 1994; Net, 2003). Intergranular volume of the Nugget and Navajo formations indicate that early compaction was considerable and far more important than cementation (Net, 2003). However, closer examination of Net's (2003) data indicates that compaction may have been more considerable within the dune facies and silica cementation more important within interdune facies. In the case of dune facies, the sediment is well sorted, which would have allowed for more rotating and slippage of grains, and hence smaller grains would go into solution easily, promoting silica precipitation (R. Q. Oaks, Jr., oral comm., 2007).

Pore space was reduced under the stress of the overburden, and the expelled pore fluids may have led to the development of feldspar and quartz overgrowths. Literature on the development of authigenic feldspar is scarce and what literature there is focuses chiefly on its development in calcareous marine sediments. Thus, the origin of authigenic feldspar is not well understood. A possible origin may be the response to groundwater flow, increasing ionic concentration in pore waters, and increased burial temperatures.

Relatively near the surface, but below the water table, initial cementation of the sediment primarily occurred by the development of incipient quartz and feldspar overgrowths, which was later followed by the precipitation calcite. Groundwater would have been ion-rich with respect to silica and/or aluminum or carbonate. As the groundwater moved through the pore system, cementation would have occurred until the pore water chemistry changed. High fluid permeability would allow the supersaturated pore waters to travel effortlessly through the sand and the high porosity would allow for large surfaces, which would allow for crystal growth.

Incipient quartz overgrowths were developed after the formation of hematite and clay coats based on the paragenetic sequences. It is unknown of the timing relation to authigenic feldspar; however, neither appears to be a major contributor to the loss of porosity. These tiny quartz overgrowths are less developed around detrital grains, which suggest a change in pore water chemistry. Also, shortly after, carbonate concretions formed. If conditions of silica supply, time, and an increase in temperature permitted, incipient quartz crystals would have developed into quartz overgrowths.

The calcite cementation typically formed concretions which are associated with coarser grained, highly porous and permeable avalanche deposits. Assuming a continuous supply of CO_2, carbonate cement will precipitate at high pH. Quartz, on the other hand, becomes more soluble at high pH. If CO_2 pressure is constant, carbonate solubility decreases with higher temperatures (Pettijohn et al., 1972). Carbonate-rich solutions may result from pressure solution of limestone. Subsequent pore water transport allows these carbonate-enriched solutions to move throughout the section. The most likely source for carbonate-saturated waters in Anschutz Ranch East field is the Twin Creek Limestone.

Mixing of natural waters within the dune field is another possible processes affecting of carbonate cementation. Waters of differing salt content, temperature, pressure, pH, or other variables, when mixed, may cause changes in the state of saturation (Runnels, 1969). This process should hold true for any mineral which forms free ions in solution; however, quartz would be affected since it dissolves to form discharge H_4SiO_4.

Petrographic criteria in thin sections indicate that secondary leached porosity generally is common to dominant in surface, near-surface, and possibly in deep subsurface sequences. Pressure solution is the most commonly described source for quartz cementation. High pressure at grain boundaries are thought to cause quartz dissolution resulting in sutured contacts. This in turn provides pore water progressively enriched in SiO_2, resulting in supersaturation and subsequent precipitation of quartz overgrowths. Although pressure solution is an attractive mechanism to explain quartz overgrowths in many cases, data presented here suggest that migrating silica-saturated waters probably supplied most of the dissolved silica for overgrowths formation. Quartz cementation is the most abundant in the lower portions of the Nugget Sandstone where there are excessive sutured contacts. However, there are certainly intervals where quartz cement is present and sutured contacts are absent (Plate 3). The absences of sutured contacts may suggest that supersaturated waters with respect to silica migrated into Anschutz Ranch East. Fox et al. (1975) concluded analogous suggestions to explain widespread quartz cementation, but lacked the sutured contacts in the Pennsylvanian Tensleep Sandstone. Because of their stability at low temperatures, supersaturated silica solutions may persist for long periods of time, thus allowing for migration over long distances (Siever, 1962; Walderhaug et al., 2000).

Aronson and Burtner (1983) used K/Ar to investigate the timing of illite authigenesis in the Nugget Sandstone in relation to migration of hydrocarbons in the Absaroka thrust sheet. The most significant results for hydrocarbon migration for Anschutz Ranch East field are from ages that were determined across the gas/oil/water contact in a producing well in Clear Creek field, which is north-northeast of Anschutz Ranch East field. The ages of the Clear Creek suite are virtually concordant at 110 ± 2 m.y. (Aronson and Burtner, 1983). Assuming hydrocarbon emplacement arrested authigenesis in the oil and gas zones, the similarity of ages from the hydrocarbon zones with the water zone indicates hydrocarbon emplacement was post 110 m.y. ago (Aronson and Burtner, 1983). Such a short lived illite authigenesis even in Clear Creek field may suggest analogous timing relationships in Anschutz Ranch East field.

The authigenic feldspar is the result of low temperature pore fluid precipitation. Present-day formation temperatures are between 20 and 30°C. Vitrinite reflectance indicates that at maximum burial depths, temperatures of about 80°C were reached in the Silurian sequence (Legall et al., 1981). The estimated depth of burial for the material used in this study, based on a geothermal gradient of 20 to 30°C/1000m, is 6562-9843 ft (2000-3000 m).

Controls on Porosity and Permeability

In order to better understand the deformational behavior of clastic rocks and resulting affects on fluid flow, the relation between rock strength and porosity is critical. Hoshino (1974) conducted a series of experimental tests on sedimentary rocks at low confining pressures and concluded that porosity is the most important mechanical factor. Therefore, understanding whether deposition or diagenesis is the main controlling factor was the fundamental issue for this study.

There are many factors in the control of the primary porosity in a clastic rock such as roundness of the grain size and sorting. In the case of the Nugget Sandstone, sand grains are nearly all well rounded to sub-angular; thus, sorting is considered as the chief depositional control on porosity. However, porosity can be reduced further through the diagenetic processes of compaction and cementation. Stephenson et al. (1992) and Net (2003) determined that the primary reduction in porosity was caused through compaction by comparing the intergranular volume (IGV) with the total amount of cement (Fig. 26). In addition, Stephenson et al. (1992) reported that compaction is the most important mechanism for reducing porosity in both well-sorted and moderately sorted samples of the Nugget Sandstone taken from Anschutz Ranch East field. This would suggest that the degree of compaction should be similar within each facies.

Stephenson et al. (1992) and Net (2003) also state that there is no significant change in the degree of compaction and/or cementation with an increase in burial depth in Anschutz Ranch East field. Petrographic analysis of the sandstone architecture accomplished in this study supports the suggestion that the degree of cementation does not change with depth. However, the type of cement does change with depth, which may have an effect on mechanical strength.

The mechanical rearrangement for sediment is dependent on initial porosity, composition, and effective stress (Giles et al., 1998). Through petrographic analysis, there were no considerable differences in the composition of Nugget Sandstone. Furthermore, the burial history of the Nugget within the study area is assumed to be fairly consistent, based on the apatite fission track and organic maturation data that Burtner and Nigrini (1994) presented. In affect the compaction of the Nugget in the study area should be consistent. Therefore, the overall trend of porosity values used in this study are interpreted to be a result of deposition, and to a lesser extent, diagenesis. Cementation generated considerable anisotropy for flow fluid and would have reduced porosity values, but that would be more on a laminae and bed scale.

Our work (Fig. 27) shows that primary depositional processes also play an important role in the porosity and permeability of the rocks. When we plot the petrophysical data in k-n space, and correlate with the depositional

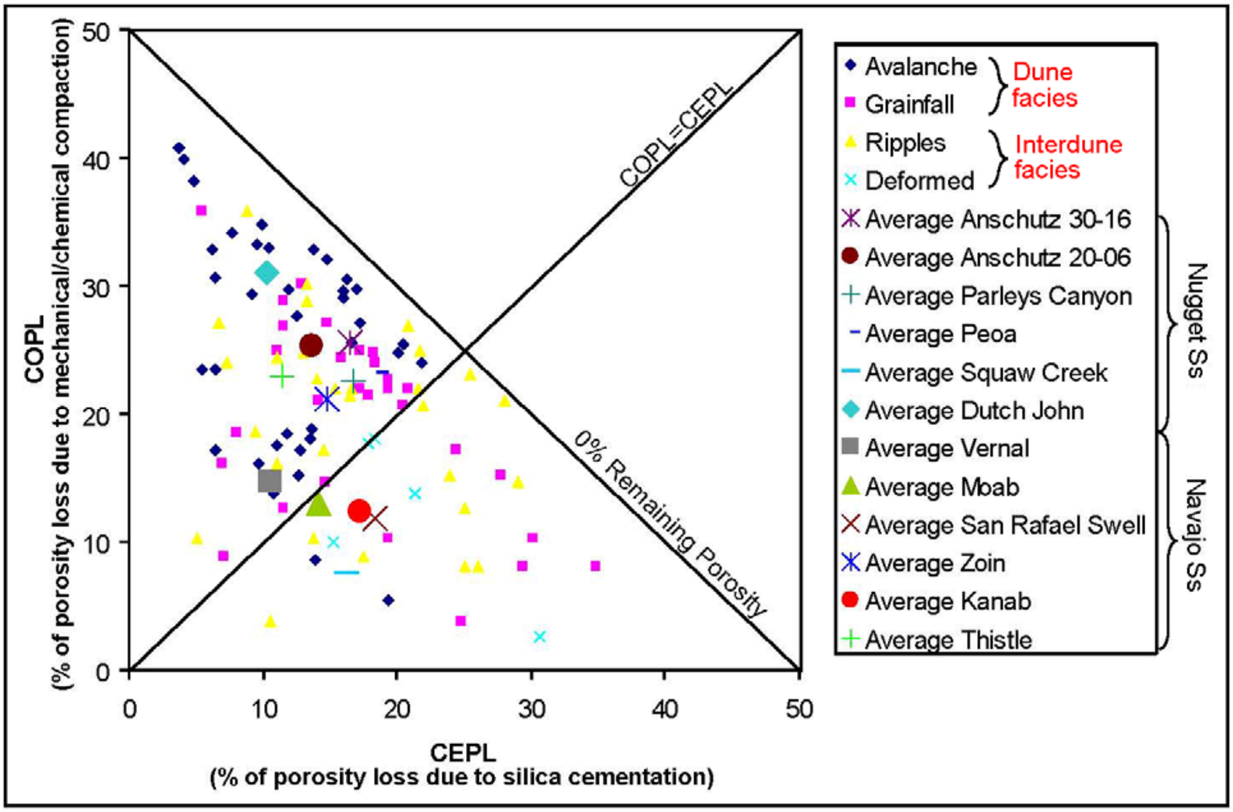

Figure 26. Relative percentages of porosity loss due to compaction and cementation for the Nugget and Navajo Sandstones. Notice that there appears to be a trend in the mechanism for porosity loss that is caused by facies. In general, dune facies will have compaction as the main mechanism for porosity loss, while interdune facies will have silica cementation as the chief mechanism. Also, notice that the Nugget has, overall, had more porosity loss than the Navajo. Modified from Net (2003).

setting inferred from the petrography, we see that the wet interdune facies have the lower k-n values, dry interdune and apron facies are intermediate, and dune facies the highest permeability and porosity. When coupled with the nature of control on deformation, we can then suggest that deformation styles produce an inverse relationship, high porosity sands tend to produce deformation bands, the low k-n rocks have open fractures and breccias, and the intermediate facies produce open to closed fractures.

Correlation Between Porosity and Style of Deformation

There is a very strong correlation between porosity in eolian rocks and the style of structural deformation that occurs. The characteristic styles of brittle deformation in the Nugget Sandstone can be separated into two intervals: interval (I) which contains the porous stratigraphic zones 1 and 2, while interval (II) contains stratigraphic zone 3, which is relatively tight compared to interval (I) (Plate 3). Zones 1 and 2 [interval (I)] are quite different in their depositional environment than zone 3 [interval (II)]. As a result, the two intervals have distinct deformational styles.

Interval (I)

In general, only deformation bands are present within interval (I). Fractures and breccia are completely absent unless a fault is

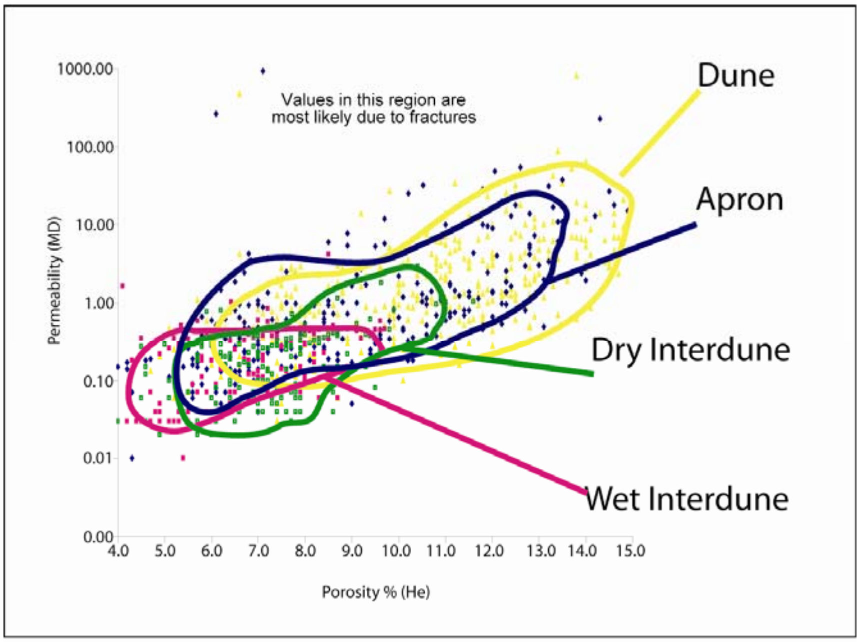

Figure 27. Nugget Sandstone facies separated into groups based on reservoir properties. In the core studied, four facies make up the Nugget. Dune facies has the highest reservoir potential. Apron facies also has a very high reservoir potential, although there are two groupings (one at the high end and one at the low end of reservoir potential). Both interdune facies are fairly low reservoir potential, however, wet interdune facies is slightly lower than dry interdune facies. Outlines (very high permeabilities) are not the result of original reservoir properties; they are the result of structural deformation (fractures).

present. The deformation bands can be interpreted as localization of slip in a porous clastic rock (Schultz and Siddharthan, 2005). In this model, porous clastic rock deforms by the compaction and shearing of grains, which reduces the grain size. As shearing continues, grain size is further reduced, which allows for fragments of the crushed grains to shift into the host rock's pore space, hence, reducing rock volume. Shifting of the grains is accomplished by rearranging their packing and leads to "yielding" which is identified with nucleation of the kinematic classes of deformation bands (Bésuelle, 2001; Schultz and Siddharthan, 2005). Aydin and Johnson (1983) suggested that deformation bands initiate at an imperfection, for example, a small volume of sandstone that contains more pore space than surrounding sandstone. This suggests that deformation bands are more likely to be seen within particular laminae, such as avalanche deposits. Our observations made during the logging of core and petrographic analysis confirm this relationship. The faults may mark a change in style of deformation from deformation bands to planner slip surfaces. Since faulting marks a change in deformation style, it would seem appropriate to consider a slip surface (a fault) as a type of mechanical instability.

Interval (II)

Deformation bands are generally absent within interval (II), while fractures and breccias are present. Interval (II) demonstrates more of a mechanical "failure" versus localized inelastic deformation yielding the growth of a deformation band. Thus, shearing of grains (grain crushing pressure) is more difficult than dilatancy (mode 1 fractures), when the host rock's porosity is too low (Schultz and Siddharthan, 2005). This observation of yielding in crystalline rocks that are very low in porosity is well documented (Scholz, 1968; Shih-Che and Harrison, 2004; Schultz and Siddharthan, 2005) even in sedimentary orthoquartzites (Schultz and Siddharthan, 2005).

Within interval (II) dilatancy and increased fracture porosity and permeability occurred. Dilatancy is an increase in volume during deformational processes. It is commonly encountered in both intact rock that is undergoing fracturing while being subject to compressive or shear stresses and pre-existing fractures that are undergoing shear displacement while being subjected to relatively low normal stresses. The orientations of fractures within interval (II) are varied and as the fracture frequency increases, fracture networks appear to be non-systematic.

CONCLUSIONS

We used a multidisciplinary approach to compare facies, diagenetic heterogeneities, style of structural deformation, and petrophysics in order to evaluate the rock properties that affect flow properties.

Facies exerts a dominant control on porosity and subsequently the strength and style of deformation of the Nugget Sandstone. Knowing that rock strength is largely a function of porosity has given rise to this study's conceptual model, which emphasizes the link between facies and structural fabric within the Nugget Sandstone in Anschutz Ranch East field. There is a hierarchical correspondence between each of the four facies (dune, apron, dry interdune, and wet interdune) and relative changes in their porosity.

In the dune facies, porosity values are generally very high, thus allowing localized deformation via the growth of deformation bands. The only style of structural heterogeneity in the dune facies is deformation bands. Because the apron facies is defined by interfingering between the dune and interdune facies, porosity values are varied, and structures include both deformation bands and fractures. In both the dry and wet interdune facies, porosity values are lower than in dune or apron facies and dilatent fractures result.

This study confirms that dune, apron, and interdune (dry and wet) facies will control variations in structural deformation styles. In addition, the present study confirmed that grain size does have an effect on porosity, but the sorting and packing of sediment have a more significant influence. Coarser-grained intervals of core do appear to be mechanically weaker and yet, coarser-grained sediment typically has sorting and packing that lead to higher porosities. Thus, this work does not consider grain size to be as important as sorting and packing. Also, interdune facies (dry and wet) do have relatively much lower porosity values and brittle failure is almost entirely the only means of structural deformation.

ACKNOWLEDGEMENTS

This report is a condensation of a M. S. thesis at Utah State University (Keele, 2008) funded by grants from the Utah Geological Survey, "Characterization of Utah's Hydrocarbon Reservoirs and Potential New Reserves" program, Association of American Petroleum Geologists (Grants-in-aid program), Society of Petrophysicists and Well Log Analysts, the Geology Department at Utah State University. Detailed descriptions, data, and photomicrographs can be found in that thesis. We thank Stephanie Carney, Tom Chidsey, and Craig Morgan of the UGS, Carol Dehler, W. David Liddell, P. T. Kolesar, and R. Q. Oaks, Jr., of Utah State University for assistance and reviews in this project.

REFERENCES

Ahlbrandt, T.S. and Fryberger, S.G., 1981, Sedimentary features and significance of interdune deposits, in Ethridge, F.P., and Flores, R.M., Recent and Ancient

Nonmarine Depositional Environments: Models for Exploration, Society of Economic Paleontologists and Mineralogists Special Publication 31, p. 293-314.

Ahlbrandt, T.S. and Fryberger, S.G., 1982, Introduction to eolian deposits, in Scholle, P.A., Spearing, D., Sandstone depositional environments: The American Association of Petroleum Geologists, Tulsa, Oklahoma, p. 11-47

Antonellini, M., and Aydin, A., 1994, Effect of faulting and fluid flow in porous sandstones: Petrophysical Properties: American Association of Petroleum Geologist Bulletin, v. 78, p. 355-377.

Aronson, J., and Burtner, R.L., 1983, K/Ar Dating of illitic clays in Jurassic Nugget Sandstone and timing of petroleum migration in Wyoming overthrust belt: Abstract, American Association of Petroleum Geology Bulletin, v. 67, 414 p.

Asquith, G., and Krygowski, D., 2004, Basic Well Log Analysis, Second Edition, The American Association of Petroleum Geologists, Tulsa, Oklahoma, 244 p.

Aydin, A., and Johnson, A. M., 1983, Analysis of faulting in porous sandstones, Jour. Of Structural Geology, v. 5, p. 19-31.

Badiozamani, K., 1973, The dorag dolomitization model, application to the middle Ordovician of Wisconsin: Journal of Sedimentary Research, v. 43, p. 965-984.

Bergosh, J.L., Good, J.R., Hillman, J.T., and Kolodzie, S., 1982, Geological characterization of the Nugget Sandstone, Anschutz Ranch East: Overthrust belt of Utah, Utah Geological Association pub. 10, p. 253-265.

Bésuelle, P., 2001, Compacting and dilating shear bands in porous rocks; theoretical and experimental conditions, Journal of Geophysical Research, v.106, pp.13,435-13,442.

Blakey, R. C.,Peterson, F. , and Kocurek, G., 1988, Syntheses of late Paleozoic and Mesozoic eolian deposits of the Western Interior of the United States, Sedimentary Geology, v. 56, p.3-125.

Brookfield, M.E., 1977, The origin of bounding surfaces in ancient eolian sandstones: Sedimentology, v. 24, p. 303-332.

Burtner, R.L., and Nigrini, A., 1994, Thermochronology of the Idaho-Wyoming thrust belt during the Sevier Orogeny: A New, calibrated, multiprocess thermal model: American Association of Petroleum Geologists, v. 78, p. 1586–1612.

Chan, M.A., Hunter, R.E., Loope, D.B., and Langford, R.P., 1992, Reflections on eolian and erg margin systems: Journal of Sedimentary Petrology, v. 62, p. 917-920.

Chan, M.A., 1999, Triassic loessite of north-central Utah; stratigraphy, petrophysical character, and paleoclimate implications: Journal of Sedimentary Research, v. 69, p. 477-485.

Coogan, J. C., 1997, Geologic map of the Sheppen Creek Quadrangle, Rich County, Utah, Utah Geological Survey Misc. Pub MP 97-2, 3 sheets, 17 pp.

Dean, W. E., Jr., 1974, Determination of carbonate and organic matter in calcareous sediments and sedimentary rocks by loss on ignition; comparison with other methods, Journal of Sedimentary Petrology, v. 44, p. 242-248.

Dickinson, W.W., and Ward, J.D., 1994, Low depositional porosity in eolian sandstone, Namib Desert: Journal of Sedimentary Research, v. A64, p. 226-232.

Dixon, J. S., 1982, Regional structural synthesis, Wyoming Salient of Western Overthrust Belt, American Association of Petroleum Geologists Bulletin, v. 66, p. 1560-1580.

Doe, T.W., and Dott, R.H., Jr., 1980, Genetic significance of deformed cross bedding-with examples from the Navajo and Weber sandstones of Utah: Journal of Sedimentary Petrology v. 50, p. 793-812.

Doelger, N.M., 1987, The stratigraphy of the Nugget Sandstone: Wyoming Geological Association Guidebook, Thrust Belts Revisited 38th Field Conference 1887, p. 163-178.

Eisenberg, L., 2003, Giant stromatolites and a supersurface in the Navajo Sandstone, Capital Reef National Park, Utah: Geology, v. 31, p. 111-114.

Fryberger, S.G., and Schenk, C.J., 1988, Pin stripe laminations: a distinctive feature of modern and ancient eolian sediments: Sedimentary Geology, v. 55, p. 1-15.

Fryberger, S.G., Ahlbrandt, T.S. and Andrews. S., 1979, Origin, sedimentary features and significance of low-angle eolian “sand sheet” deposits, Great Sand Dunes National Monument and vicinity, Colorado: Journal of Sedimentary Petrology, v. 49, p. 733-746.

Füchtbauer, H., 1967, Influence of different types of diagenesis on sandstone porosity: 7th World Petroleum Congress Proceedings, v. 2, p. 353-369.

Fox, J.E., Lambert, P.W., Mast, R.F., Nuss, N.W., and Rein, R.D, 1975, Porosity variation in the Tensleep and its equivalent the Weber sandstone, Western Wyoming: A log and petrographic analysis, in Rocky Mountain Association of Geologists, 1975 symposium, p. 185-216.

Giles, M. R., Indrelid, S. L., and James, D. M. D., 1998, Compaction — the great unknown in basin modeling, Geological Society, London, Special Publications, v. 141, p. 15-43.

Heward, A.P., 1991, Inside Auk – the anatomy of an eolian oil reservoir, in Miall, A.D. and Tyler, N. (Eds.), The Three-Dimensional Facies Architecture of Terrigenous Clastic Sediments and its Implications for Hydrocarbon Discovery and Recovery. SEPM Concepts in Sedimentology and Paleontology, v. 3 p. 44-56.

Hoshino, K., 1974, Effect of porosity on the strength of the clastic sedimentary rocks: Proceedings of the Third Congress of the International Society for Rock Mechanics, v. 2, part A, Denver, Colorado, September 1-7, 1974, p. 511-516.

Hummel, G., and Kocurek, G., 1984, Interdune areas of the back-island dune field, North Padre Island, Texas: Sedimentary Geology, v. 39, p. 1–26.

Hunter, R.E., 1977, Basic types of stratification in small eolian dunes: Sedimentology, v. 24, p. 361-387.

Hunter, R.E., 1981, Stratification styles in eolian sandstone: some Pennsylvanian to Jurassic examples from the western interior, USA: Special Publication Society of Economic Paleontologists and Mineralogists, v. 31, p. 315-329.

Ingersoll, R.V., Bullard, T.F., Ford, R.L., Grimm, J.P., Pickle, J.D., and Sares, S.W., 1984, The effect of grain size on detrital modes: A test of the Gazzi-Dickson point counting method: Journal of Sedimentary Petrology, v. 54, p. 103-116.

Jordan, W.M., 1965, Regional environmental study of the early Mesozoic Nugget and Navajo sandstones[Ph.D. Dissertation]: Madison, Wisconsin, University of Wisconsin, 206 p.

Kleinsteiber, S.W., Wendschlag, D.D., and Calvin, J.W., 1983, A study for development of a depletion in a rich gas condensate reservoir: Anschutz Ranch East unit, Summit County, Utah Uinta County, Wyoming: Society of Petroleum Engineers, SPE 12042, 58th Annual Technical Conference, San Francisco, Oct. 5-8, 1983, 11 p.

Kocurek, G., 1981, Significance of interdune deposits and bounding surfaces in eolian sand dunes: Sedimentology, v. 28, p. 753-780.

Kocurek, G., and Hunter, R.E., 1986, Origin of Polygonal fractures in sand, uppermost Navajo and Page sandstones, Page, Arizona: Journal of Sedimentary Petrology, v. 56, p. 895-904.

Kocurek, G., Havholm, K.G., 1993. Eolian sequence stratigraphy— a conceptual framework. In: Weimer, P., Posamentier, H., Recent advances in and applications of siliciclastic sequence stratigraphy. American Association of Petroleum Geologists Memoir 58, pp. 393–409.

Kulander, B.R., Dean, S.L., and Ward, Jr. B.J., 1990, Fractured Core Analysis: Interpretations, Logging, and Use of Natural and Induced Fractures in Core: Association American Petroleum Geologist Series, no. 8, The American of Association of Petroleum Geologists, Tulsa, Oklahoma, 148 p.

Lamerson, P.R., 1982, Fossil basin area and it's relationship to the Absaroka thrust fault system, in Powers, R.B. Geologic Studies of the Cordilleran Thrust belt. Rocky Mountain Association of Geologists, Denver, v. 1, p. 279-340.

Lancaster, N., 1981, Grain size characteristics of Namib Desert linear dunes: Sedimentology, v. 28, p. 115-122.

Legall, F.D., Barnes, C.R. and MacQueen, R.W. 1981. Thermal maturation, burial history and hotspot development, Paleozoic strata of southern Ontario-Quebec, from conodont and acritarch colour alteration studies, Bulletin of Canadian Petroleum Geology, v. 29, p. 492-539.

Lelek, J.J., 1982, Anschutz Ranch field, northeast Utah and southwest Wyoming, in Powers, R.B. Geologic Studies of the Cordilleran Thrust belt. Rocky Mountain Association of Geologists, Denver, v. 2, p. 619-631.

Lelek, J.J., 1983, Geologic factors affecting reservoir Analysis, Anschutz East Field, Utah and Wyoming: Journal of Petroleum Technology, v. 35, p. 1539-1545.

LeTourneau, P.M., and Hiber, P., 2006, Early Jurassic eolian dune field, Pomperaug basin, Connecticut and related synrift deposits: Stratigraphic framework and paleoclimatic context: Sedimentary Geology, v. 187, p. 63-81.

Lewis, H., and Couples, G.D., 1993, Production evidence for geological heterogeneities in Anschutz Ranch East field, western USA, in: North, C.P., and Prosser, D.J. (Eds.) Characterization of Fluvial and Eolian Reservoirs: Geological Society Special Publication, v. 73, p. 321-338.

Lindquist, S.J., 1983, Nugget Sandstone reservoir characteristics affecting production in the overthrust belt of southwest Wyoming: Journal of Petroleum Technology, v. 35, p. 1355-1365.

Lindquist, S.J., 1988, Practical characterization of eolian reservoirs for development: Nugget Sandstone, Utah-Wyoming thrust belt: Sedimentary Geology, v. 56. p. 315-339.

Loope, D.B., Steiner, M. B.,Rowe, C. M., and Lancaster, N., 2004, Tropical westerlies over Pangaean sand seas, Sedimentology, v. 51, p. 315-322.

McBride, E.F., Land, L.S., and Mack, L.E., 1987, Diagenesis of eolian and fluvial feldspathic sandstones, Norphlet Formation (upper Jurassic), Rankin County, Mississippi, and Mobile County, Alabama: The American Association of Petroleum Geologists, v. 71, p. 1019-1034.

McKee, E.D., and Tibbets, G.C., 1964, Primary structures of a seif dune and associated deposits in Libya: Journal of Sedimentary Geology, v. 34, p. 5-17.

McKee, E.D., 1971, Deformation of lee-side laminae in eolian dunes: Geological Society of America Bulletin, v. 82, p. 359-378.

McKee, E.D., and Bigarella, J.J., 1979, Sedimentary structures in dunes, with sections on the Lagoa dune field, Brazil, *in* McKee, E.D., ed., A study of gobal Sand Seas, U.S. Geological Survey Professional Paper 1052, p. 83-139.

Mountney, N., and Howell, J., 2000, Eolian architecture, bedform climbing and preservation space in the Cretaceous Etjo Formation, NW Namibia: Sedimentology, v. 47, p. 825-849.

Mountney, N.P. and Thompson, D.B., 2002, Stratigraphic evolution and preservation of eolian dune and damp/wet interdune strata: an example from the Triassic Helsby sandstone Formation, Cheshire basin, UK: Sedimentology, v. 49, p. 805-833.

Morse, D. G., 1994, Siliciclastic reservoir rocks, in: Magoon, L. B., Dow, W. G., The petroleum system; from source to trap: American Association Petroleum Geologists, Memoir, 60, p. 121-139.

Nelson, R.A., 2001, Geologic Analysis of Naturally Fractured Reservoirs, Gulf Professional Publishing, Woburn, Massachusetts, 332 p.

Net, L.I., 2003, Diagenesis and Reservoir Quality of the Eolian Nugget / Navajo Sandstone (Early Jurassic), Utah and Wyoming, [M.S. Thesis]: Austin, Texas, University of Texas at Austin, 182 p.

Paxton, S.T., Szabo, J.O., Ajdukiewicz, J.M., and Klimentidis, R.E., 2002, Construction of intergranular volume compaction curve for evaluating and predicting compaction and porosity loss in rigid-grain sandstone reservoirs: American Association of Petroleum Geologist Bulletin, v. 86, p. 2047-2067.

Peterson, F., 1988, Pennsylvanian to Jurassic eolian tranporation systems in the western United States: Sedimentary Geology, v. 56, p. 207-260.

Peterson, F., and Pipiringos, G.N., 1979, Stratigraphic relations of the Navajo Sandstone to middle Jurassic formations, southern Utah and northern Arizona: United States Geological Survey, Professional Paper, v. 1035-B, 43 p.

Pettijohn, F.A., Potter, P.E., and Siever, R., 1972, Sand and sandstone. Springer-Verlag, New York, 618 p.

Price, R.A., 1967, The tectonic significance of mesoscopic subfabrics in the southern Rocky Mountains of Alberta and British Columbia: Can. Journal of Earth Science, v. 4, p. 39-70.

Runnels, D.D., 1969, Diagenesis, chemical sediments, and the mixing of natural waters: Journal of Sedimentary Petrology, v. 39, p. 1188-1201.

Salvini, F., and F. Storti, 2004, Active-hinge-folding-related deformation and its role in hydrocarbon exploration and development—Insights from HCA modeling, in K. R. McClay, ed., Thrust tectonics and hydrocarbon systems: American Association of Petroleum Geologists Memoir 82, p. 453– 472.

Schenk, C.S., 1983, Textural and structural characteristics of some experimentally formed eolian strata, in Brookfield, M.E., and Ahlbrandt, T.S., Eolian sediments and processes. Developments in sedimentary, v. 38, p. 41-49.

Schenk, C.S., 1990, Core examples of eolian sandstone, in Fryberger, S.G., Modern and ancient eolian deposits: Petroleum Exploration and Production, Society of Sedimentary Geology, Denver, Colorado.

Shih-Che Yuan and J. P. Harrison, 2004, An empirical dilatancy index for the dilatant deformation of rock: International Journal of Rock Mechanics and Mining Sciences, v. 41, p. 679-686.

Siever, R., 1962, Silica solubility, 0°-200°C and the diagenesis of siliceous sediments: Journal of Geology, v. 70, p. 127-150.

Scholz, C. H., 1968, Experimental study of the fracturing process in brittle rock, Journal of Geophysical Research,

v.73, pp.1447-1454.
Schultz, R.A., and Siddharthan, R., 2005, A general framework for the occurrence and faulting of deformation bands in porous granular rocks: Tectonophysics, v. 411, p. 1-18.
Stanistreet, I.G., and Stollhofen, H., 2002, Hoanib River flood deposits of Namib Desert interdunes as analogues for thin permeability barrier mudstone layers in eolianite reservoirs: Sedimentology, v. 49, p. 719–736.
Stephenson, L.P., Plummley, W.J., and Palciauskas, V.V., 1992, A model for sandstone compaction by grain interaction: Journal of Sedimentary Petrology, v. 62, p. 11-22.
Sweet, M.L., Weilson, J., Havholm, K., Farrelley, John, 1988, Algodones dune field of southeastern California; case history of a migrating modern dune field: Sedimentology, vol. 35, p. 939-952.
Walderhaug, O., Lander, R.H., Bjørkim, P.A., Oelkers, E.H., Bjørlykke, K., and Nadeau, P.H., 2000, Modelling quartz cementation and porosity in reservoir sandstone: examples from the Norweian continental shelf: Quartz cementation in sandstones, n.29, Blackwell Science, p. 39-50.
Warner, M.A., 1982, Generation of hydrocarbons-Fossil basin, in Powers, R.B. Geologic Studies of the Cordilleran Thrust belt. Rocky Mountain Association of Geologists, Denver, v. 2, p. 805-830.
West, J., and Lewis, H., 1982, Structure and palinspastic reconstruction of the Absaroka thrust, Anschutz Ranch area, in Powers, R.B. Geologic Studies of the Cordilleran Thrust belt. Rocky Mountain Association of Geologists, Denver, v. 2, p. 633-639.
White, R.R., Alcock, T.J., and Nelson, R.A., 1990, Anschutz Ranch East Field U.S.A.; Utah-Wyoming thrust belt, in: Beaumont, E.A., and Foster, N.H. (Eds.), Structural traps; III, Tectonic fold and fault traps. APPG Treatise of Petroleum Geology, Atlas of Oil and Gas Fields, v. A-019, p. 31-55.
Wilson, M.D., and Stanton, P.T., 1994, Diagenetic mechanisms of porosity and permeability reduction and enhancement, Reservoir quality assessment and prediction in clastic rocks: Society of Sedimentary Geology, Short Course, v. 30, p. 59-118.
Worden, R.H., and Morad, S., 2003, Clay minerals in sandstones: controls on formation, distribution and evolution: International Association of Sedimentologists, v. 34, p. 3-41.

Plate 1. Geologic Map of South Eden Canyon, Rich County, Utah

475889E
4641889N

478825E
4641889N

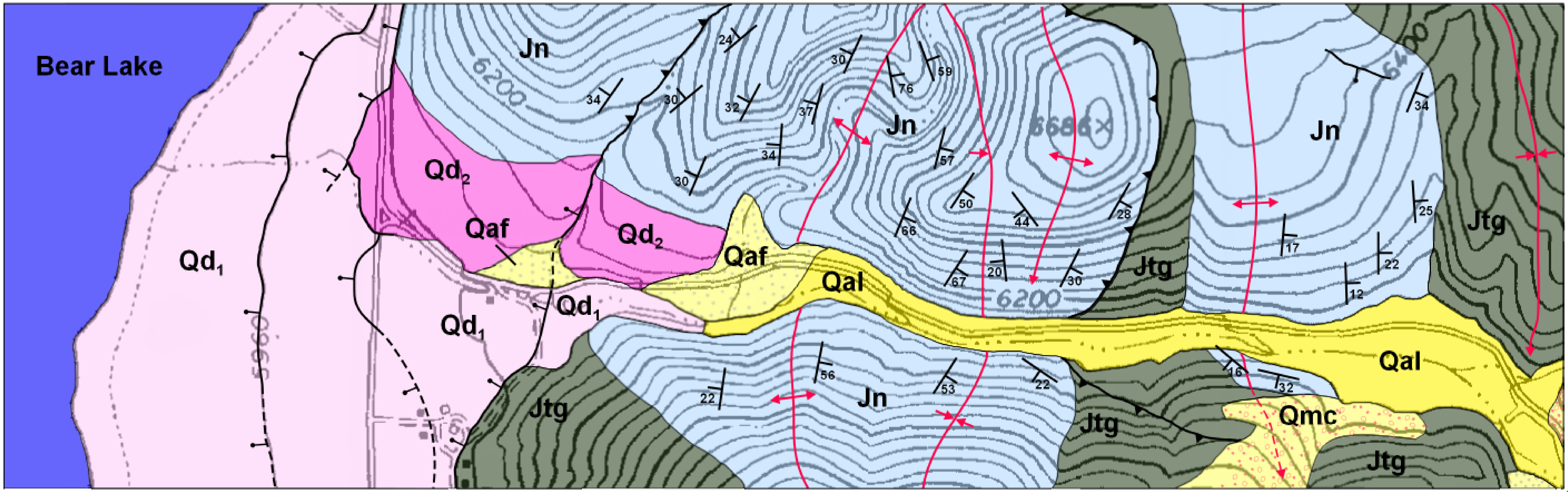

475885E
4641024N

478825E
4641024N

1000 750 500 250 0 METERS

3500 3000 2500 1500 1000 500 0 FEET

1000 meters

CONTOUR INTERVAL 20 FEET

SCALE 1 : 50000

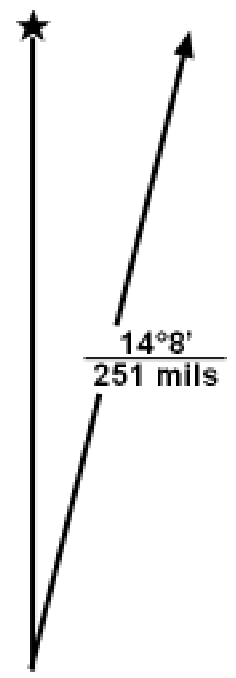

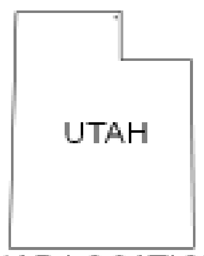

Modified from Coogan, J.C., 1997, Geologic Map of Bear Lake South Quadrangle, Rich County, Utah: Utah Geological Survey Miscellaneous Publication 97-1, scale 1:24000, Plate 1.

Contact - solid line where known contact is located; dashed line where approximately located; dotted line where concealed

Normal Fault - ball and bar on downthrown side

Thrust Fault - sawteeth on upper plate

Anticline

Monocline

Syncline

DESCRIPTION OF MAP UNITS

Qal	Alluvium - Gravel, sand, silt, and mud in valley bottoms of streams.
Qaf	Younger alluvial-fan deposits - Poorly sorted, clay to boulder-sized material in crudely stratified, fan-shaped deposits.
Qd_1	Younger deltaic deposits - Gravel, sand, and silt capped by loess in delta-shaped exposures along Bear Lake; deposits are crudely stratified, and include two linear ridges of sand and gravel.
Qd_2	Older deltaic deposits - Crudely stratified gravel, sand, and silt apparently deposited in alluvial fans and at lower elevations in deltas in Bear Lake
Qmc	Colluvium - Angular, silt to boulder-sized material from nearby outcrops.
Jtg	Gypsum Springs Member of Twin Creek Limestone - Red shale, siltstone, and sandstone; gray dolomite and brecciated dolomite; anhydrite in subsurface.
Jn	Nugget Sandstone - Red-Orange, friable, medium to fine-grained, quartz sandstone; capping by white, well-indurated sandstone is common.

Plate 2. Geologic Map of North Eden Canyon, Rich County, Utah

479405E
4648788N

483217E
4648788N

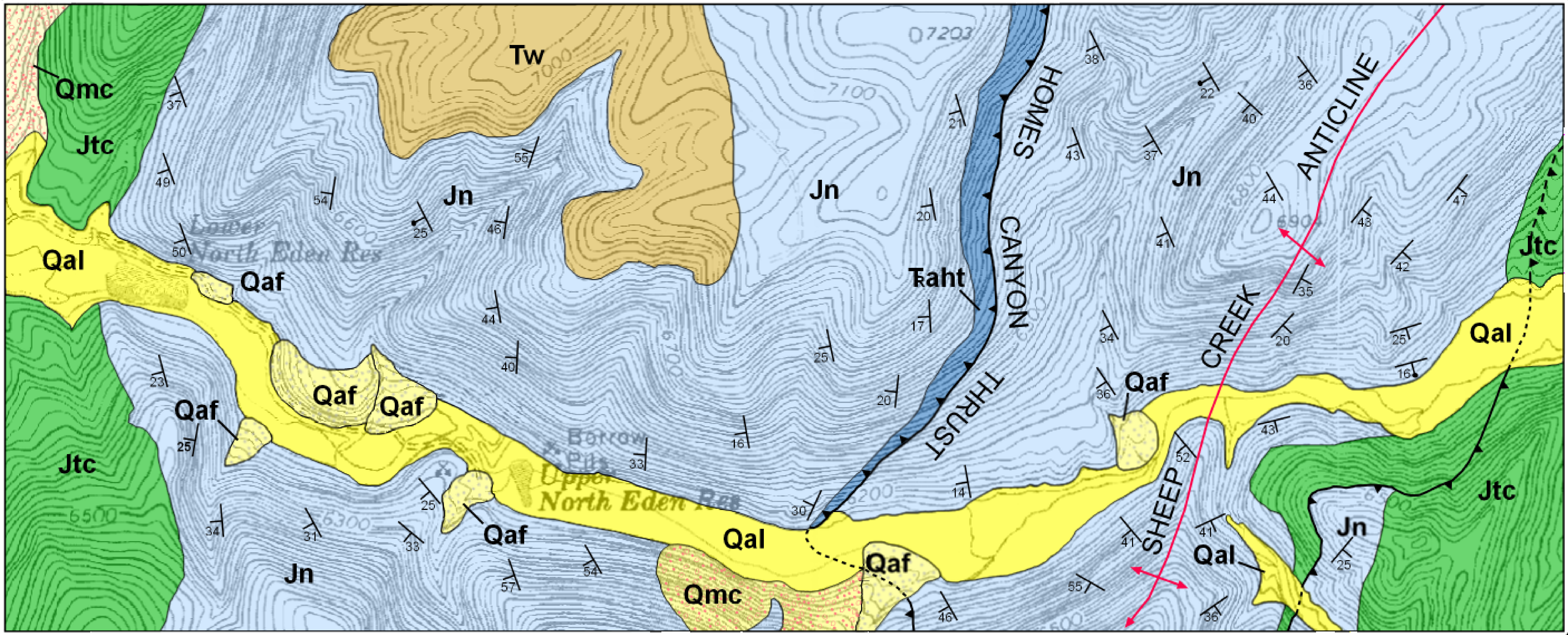

479405E
4647323N

483217E
4647323N

1000 750 500 250 0 METERS

3500 3000 2500 1500 1000 500 0 FEET

CONTOUR INTERVAL 20 FEET

SCALE 1 : 50000

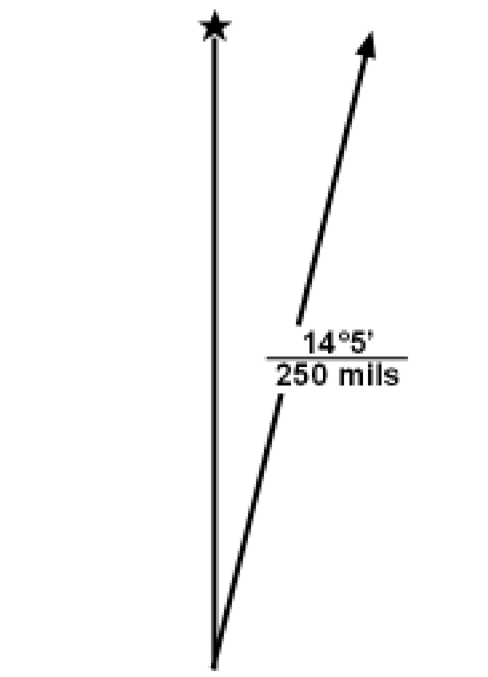

1997 MAGNETIC DECLINATION

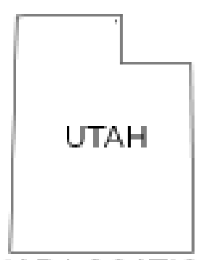

MAP LOCATION

Modified from Coogan, J.C., 1997, Geologic Map of Sheep Creek Quarangle, Rich County, Utah: Utah Geological Survey Miscellaneous Publication 97-2, scale 1:24000, Plate 1.

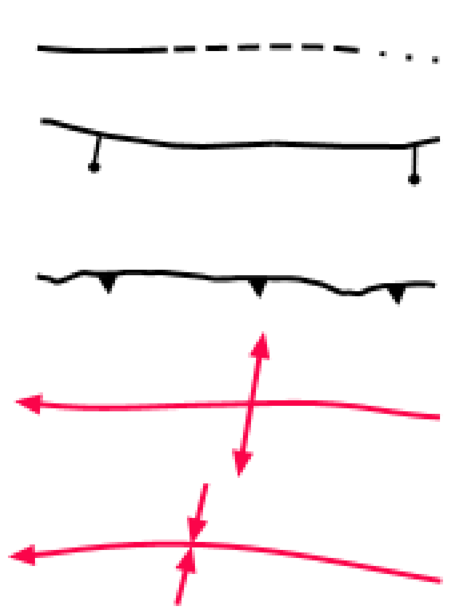

Contact - solid line where known contact is located; dashed line where approximately located; dotted line where concealed

Normal Fault - ball and bar on downthrown side

Thrust Fault - sawteeth on upper plate

Anticline

Syncline

DESCRIPTION OF MAP UNITS

Qal Alluvium - Gravel, sand, silt, and mud in valley bottoms of streams.

Qaf Younger alluvial-fan deposits - Poorly sorted, clay to boulder-sized material in crudely stratified, fan-shaped deposits.

Qmc Colluvium - Angular, silt to boulder-sized material from nearby outcrops.

Tw Main body of the Wasatch Formation - Poorly exposed red mudstone, and lesser sandstone and conglomerate.

Jtc Twin Creek Limestone - Red shale, siltstone, and sandstone; gray lime packstone with pencil cleavage, wackestone, and grainstone with fossils.

Jn Nugget Sandstone - Red-orange, friable, medium to fine-grained, quartz sandstone; capping by white, well-indurated sandstone is common.

Ŧaht Ankareh Formation - Red-tan, siltsone and sandstone, grey-brown, shale and limestone.

Plate 3. Compilation logs of the ARE 30-02, 29-04ST, and 20-16 wells from Anschutz Ranch East field, Utah.

Lithology logs from logging of core by Dustin Keele. Core is stored at the Oklahoma Geologic Survey, Norman. Porosity and permeability data from petrophysical data collected by CoreLabs, for Amoco, Inc., and on file at the Utah Division of Oil, Gas and Mining.

Facies	Lithologic characteristics	Diagenetic features	Depositional system
Dune	Very fine -medium grain size, High-angle cross-strata, Low-amplitude ripples	Buff color, Calcite nodules, Carbonate rich beds, Desert varnish, Hydrocarbon staining along coarse beds	Erg
Apron	Very fine -medium grain size, High-angle cross-strata, Low-amplitude cross strata, Low-amplitude ripples, Horizontal beds	Buff color, Calcite nodules, Carbonate rich beds, Desert varnish, Hydrocarbon staining along coarse beds	Erg/Sandsheet
Dry Interdune	Silt -very fine grain size, Low-amplitude ripples, Horizontal beds	Hematite staining	Sandsheet
Wet Interdune	Silt -very fine grain size, Soft-sediment deformation, Bioturbation, High-amplitude ripples, Thin horizontal beds, Trough cross strata, Carbonate rich horizons, Scoured surfaces, Mudstone, Convoluted beds	Hematite staining	Interdune/Sabkha